Supporting Information for

Chain-Walking Polymerization of Linear Internal Octenes Catalyzed by *α*-Diimine Nickel Complexes

Fuzhou Wang,*[,†,‡] Ryo Tanaka,[‡] Qingshan Li,[§] Yuushou Nakayama,[‡] and Takeshi Shiono*[,‡]

[†]Institute of Physical Science and Information Technology, Anhui University, Hefei 230601, Anhui, China.

[‡]Graduate School of Engineering, Hiroshima University, Kagamiyama 1-4-1, Higashi-Hiroshima 739-8527, Japan.

[§]Department of Chemistry, Nankai University, Tianjin 300071, China.

*E-mail: wangfuzhou1718@126.com (F. W); tshiono@hiroshima-u.ac.jp (T. S)

Table of contents

1. Synthesis and characterization

2.1. Synthesis of *α*-diimine ligands L1–L6 and complexes 1–6

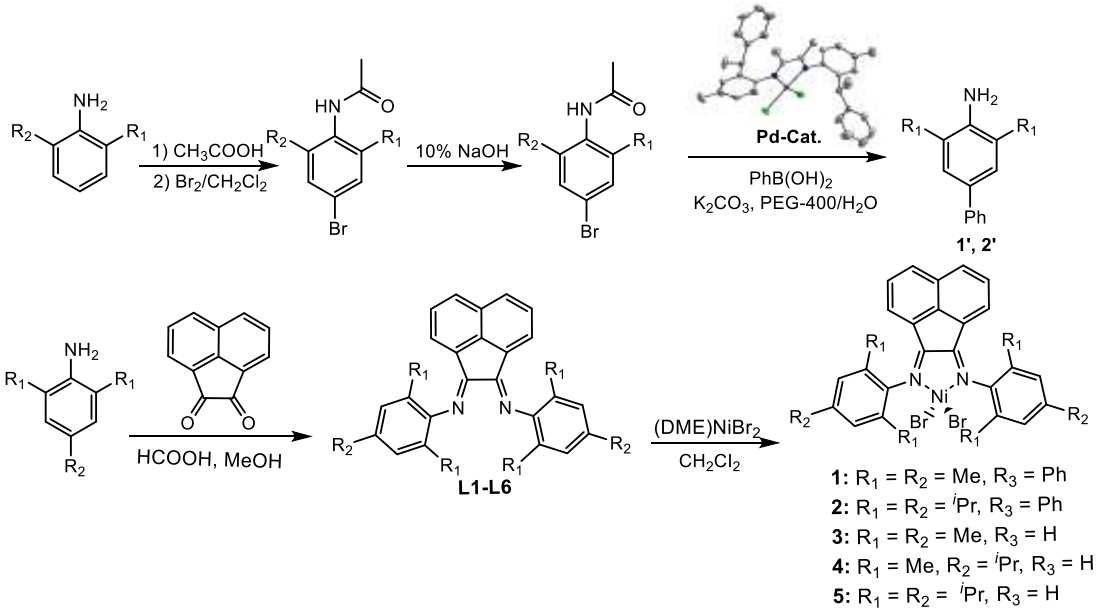

Scheme S1. Synthesis of *α*-diimine ligands **L1–L6** and their complexes **1–6**.

The synthesis of *α*-diimine ligands **L1–L6** and complexes **1–6** are outlined in Scheme S1. The ligands are accessible by a three-step procedure. After protection of the amino group by acetic acid, 4-H-anilines were brominated to form aniline bromides. The Suzuki-coupling reaction of 4-bromo-substituted-anilines and phenylboronic acid catalyzed by **Pd-Cat**., in PEG-400, led to the corresponding 4-phenyl-substituted-anilines **1′** and **2′** [1]. The ligands **L1–L6** were prepared by the condensation of equivalents of the appropriate aniline with one equivalent of acenaphthoquinone, usually in the presence of a formic acid as a catalyst. Compounds **L1–L6** were well characterized by IR, $\{^1H\}^{13}C$ NMR spectroscopy and elemental analysis.

The reaction of equimolar amounts of $NiBr_2$(DME) and the *α*-diimine ligands in CH_2Cl_2 led to the displacement of 1,2-dimethoxyethane and afforded the catalyst precursors **1–6** as a moderately air-stable deep red microcrystalline solid in almost quantitative yield. These complexes were characterized by IR spectroscopy and elemental analysis.

Synthesis of aniline derivatives

*Synthesis of 2,6-dimethyl-4-phenylaniline **1′***

4-Bromo-2,6-dimethylaniline (0.40 g, 2.00 mmol), phenylboronic acid (0.26 g, 2.10 mmol), K_2CO_3 (0.55 g, 4.00 mmol) and Pd-Cat. (0.026 g, 0.04 mmol), were placed in a 100-mL flask and allowed to stir at room temperature for 12 h, in the presence of PEG-400/H_2O (30 mL/1.0 mL). The mixture was extracted three times with 10 mL diethyl ether. The combined organic phase was dried over $MgSO_4$, filtered, and the solvent was removed. The residue was purified by chromatography on silica gel with

petroleum ether/ethyl ester (v/v = 25:1) to give 2,6-dimethyl-4-phenylaniline **1′** (0.34 g, 86% yield). ^{1}H NMR (400 MHz, $CDCl_3$, ppm): δ 7.45−7.50 (m, 2H, Ar−*H*), 7.28−7.35 (m, 2H, Ar−*H*), 7.13−7.21 (m, 3H, Ar−*H*), 3.54 (s, 2H, −N*H*$_2$), 2.15 (s, 6H, −C*H*$_3$). ^{13}C NMR (400 MHz, $CDCl_3$, ppm): δ 142.22, 141.41, 130.90, 128.50, 126.93, 126.42, 125.98, 121.90, 17.73 (−*C*H$_3$).

*Synthesis of 2,6-diisopropyl-4-phenylaniline **2′***

Using the same synthetic procedure for **1′**, **2′** was obtained as an oily liquid (0.41 g, 81% yield). ^{1}H NMR (400 MHz, $CDCl_3$, ppm): δ 7.46−7.56 (m, 2H, Ar−*H*), 7.34−7.40 (m, 2H, Ar−*H*), 7.29 (s, 2H, Ar−*H*), 7.25 (t, *J* = 8.0 Hz, 1H, Ar−*H*), 3.79 (s, 2H, −N*H*$_2$), 2.95−2.98 (m, 2H, −C*H*(CH$_3$)$_2$), 1.33 (d, *J* = 7.8 Hz, 12H, −C*H*$_3$). ^{13}C NMR (400 MHz, $CDCl_3$, ppm): δ 142.45, 132.68, 131.41, 128.62, 126.61, 125.96, 125.72, 121.92, 28.07 (−C*H*(CH$_3$)$_3$), 22.43 (−*C*H$_3$).

*Synthesis of ligands **L1**, **L3**, **L5** and **L6***

*Synthesis of bis[N, N′-(2,6-dimethyl-4-phenylphenyl)imino]acenaphthene **L1***

Formic acid (0.2 mL) was added to a stirred solution of 1,2-acenaphthylenedione (0.091 g, 0.50 mmol) and 2,6-dimethyl-4-phenylaniline (0.22 g, 1.10 mmol) in MeOH (30 mL). The mixture was refluxed for 12 h, then cooled and the precipitate was separated by filtration. The solid was recrystallized from MeOH/CH_2Cl_2 (v/v = 14:1), washed with cold ethanol and dried under vacuum (0.22 g, 80 % yield). ^{1}H NMR (400 MHz, $CDCl_3$, ppm): δ 7.92 (d, *J* = 8.0 Hz, 2H, Nap−*H*), 7.70−7.79 (m, 4H, Nap−*H* and Ar−*H*), 7.41−7.49 (m, 8H, Ar−*H*), 7.35−7.39 (m, 4H, Ar−*H*), 6.87 (d, *J* = 7.2 Hz, 2H, Nap−*H*), 2.22 (s, 12H, −C*H*$_3$). ^{13}C NMR (400 MHz, $CDCl_3$, ppm): δ 160.99 (*C*═N), 148.64, 140.97, 140.65 (Nap−*C*), 136.35, 131.05 (Nap−*C*), 129.58, 129.02 (Nap−*C*), 128.69, 128.32 (Nap−*C*), 126.93, 126.79, 126.71, 125.28 (Nap−*C*), 122.64 (Nap−*C*), 17.99 (−*C*H$_3$). Anal. Calcd. for $C_{40}H_{32}N_2$: C, 88.85; H, 5.97; N, 5.18. Found: C, 88.91; H, 6.02; N, 5.14. FT-IR (KBr): 1640 cm^{-1} ($\nu_{C=N}$).

*Synthesis of bis[N, N′-(2,6-diimethylphenyl)imino]acenaphthene **L3***

Using the same synthetic procedure for **L1**, **L3** was obtained as a yellow–orange powder (0.27 g, 86% yield). ^{1}H NMR (400 MHz, $CDCl_3$, ppm): δ 7.89 (d, *J* = 8.2 Hz, 2H, Nap−*H*), 7.39 (t, *J* = 7.8 Hz, 2H, Nap−*H*), 6.98−7.21 (m, 6H, Ar−*H*), 6.69 (d, *J* = 7.2 Hz, 2H, Nap−*H*), 2.16 (s, 12H, −C*H*$_3$). ^{13}C NMR (400 MHz, $CDCl_3$, ppm): δ 161.2, 149.5, 140.9, 131.3, 129.8, 129.3, 128.5, 128.6, 125.0, 124.0, 122.8, 18.1 (−*C*H$_3$). Anal. Calcd. for $C_{28}H_{24}N_2$: C, 86.56; H, 6.23; N, 7.21. Found: C, 86.68; H, 6.19; N, 7.12. FT-IR (KBr): 1,635 cm^{-1} ($\nu_{C=N}$).

*Synthesis of bis[N, N′-(2,6-diisopropylphenyl)imino]acenaphthene **L5***

Using the same synthetic procedure for **L1**, **L5** was obtained as an red powder (0.22 g, 87% yield). ^{1}H NMR (400 MHz, $CDCl_3$, ppm): δ 7.88 (d, *J* = 8.0 Hz, 2H, Nap−*H*), 7.36 (t, *J* = 8.0 Hz, 2H, Nap−*H*), 7.24−7.30 (m, 6H, Ar−*H*), 6.63 (d, *J* = 7.2 Hz, 2H, Nap−H), 3.00−3.07 (m, 4H, −C*H*(CH$_3$)$_2$), 1.23 (d, *J* = 6.8 Hz, 12H, −C*H*$_3$), 0.97 (d, *J* = 6.8 Hz, 12H, −C*H*$_3$). ^{13}C NMR (400 MHz, $CDCl_3$, ppm): δ 160.92, 147.44, 140.75, 135.37, 130.94, 129.44, 128.83, 127.83, 124.25, 123.43, 28.58 (−C*H*(CH$_3$)$_3$), 23.10

(−CH_3). Anal. Calcd. for $C_{36}H_{40}N_2$: C, 86.35; H, 8.05; N, 5.59. Found: C, 86.37; H, 7.98; N, 5.63. FT-IR (KBr): 1634 cm^{-1} ($\nu_{C=N}$).

*Synthesis of bis[N, N′-(2,6-diisopropylphenyl)imino]acenaphthene **L6***

Using the same synthetic procedure for **L1**, **L6** was obtained as an red powder (0.25 g, 75% yield). ^{1}H NMR (400 MHz, $CDCl_3$, ppm): δ 7.93 (d, J = 8.2 Hz, 2H, Nap−*H*), 7.44 (t, J = 7.8 Hz, 2H, Nap−*H*), 7.39 (s, 4H, Ar−*H*), 6.77 (d, J = 7.2 Hz, 2H, Nap−*H*), 2.92−2.99 (m, 4H, −C*H*(CH_3)$_2$), 1.20 (d, J = 6.8 Hz, 12H, −C*H*$_3$), 0.94 (d, J = 6.8 Hz, 12H, −C*H*$_3$). ^{13}C NMR (400 MHz, $CDCl_3$, ppm): δ 161.22, 146.31, 140.90, 137.87, 129.22, 128.04, 126.82, 123.44, 117.76, 112.06, 28.77 (−C*H*(CH_3)$_3$), 23.02 (−*C*H_3). Anal. Calcd. for $C_{36}H_{38}Br_2N_2$: C, 65.66; H, 5.82; N, 4.25. Found: C, 65.49; H, 5.76; N, 4.21. FT-IR (KBr): 1,631 cm^{-1} ($\nu_{C=N}$).

*Synthesis of complexes **1**, **3** and **5–7***

*Synthesis of {bis[N,N′-(2,6-dimethyl-4-phenylphenyl)imino]acenaphthene}dibromonickel **1***

[(DME)$NiBr_2$] (0.16 g, 0.50 mmol) and **L1** (0.28 g, 0.50 mmol) were combined in a Schlenk flask under a N_2 atmosphere. CH_2Cl_2 (20 mL) was added, and the reaction mixture was stirred at room temperature for 24 h. The resulting suspension was filtered. The solvent was removed under vacuum and the residue was washed with diethyl ether (3 × 15 mL), and then dried under vacuum at room temperature to give nickel complex **1** (0.33 g, 86 % yield). Anal. Calcd. for $C_{40}H_{32}Br_2N_2Ni$: C, 63.28; H, 4.25; N, 3.69. Found: C, 63.34; H, 4.30; N, 3.75. FT-IR (KBr): 1639 cm^{-1} ($\nu_{C=N}$). Single crystals of complex **1** suitable for X-ray analysis were obtained at room temperature by dissolving the nickel complex in CH_2Cl_2, following by slow layering of the resulting solution with *n*-hexane.

*Synthesis of {bis[N, N′-(2,6-dimethylphenyl)imino]acenaphthene}dibromonickel **3***

Using the same synthetic procedure for **1**, **3** was obtained as a dark-red powder (0.26 g, 85 % yield). Anal. Calcd. for $C_{28}H_{24}Br_2N_2Ni$: C, 55.40; H, 3.99; N, 4.62. Found: C, 55.31; H, 3.93; N, 4.65. FT-IR (KBr) 1,647 cm^{-1} ($\nu_{C=N}$).

*Synthesis of {bis[N, N′-(2,6-diisopropylphenyl)imino]acenaphthene}dibromonickel **5***

Using the same synthetic procedure for **1**, **5** was obtained as a dark-red powder (0.34 g, 95 % yield). Anal. Calcd. for $C_{36}H_{40}Br_2N_2Ni$: C, 60.12; H, 5.61; N, 3.89. Found: C, 56.69; H, 4.49; N, 4.38. FT-IR (KBr) 1,642 cm^{-1} ($\nu_{C=N}$).

*Synthesis of {bis[N, N′-(4-bromo-2,6-diisopropylphenyl)imino]acenaphthene}dibromonickel **6***

Using the same synthetic procedure for **1**, **6** was obtained as a dark-red powder (0.40 g, 91 % yield). Anal. Calcd. for $C_{36}H_{38}Br_4N_2Ni$: C, 49.30; H, 4.37; N, 3.19. Found: C, 49.67; H, 4.33; N, 3.15. FT-IR (KBr) 1,641 cm^{-1} ($\nu_{C=N}$).

1.2. ^{1}H and ^{13}C NMR spectra of ligands L1–L6

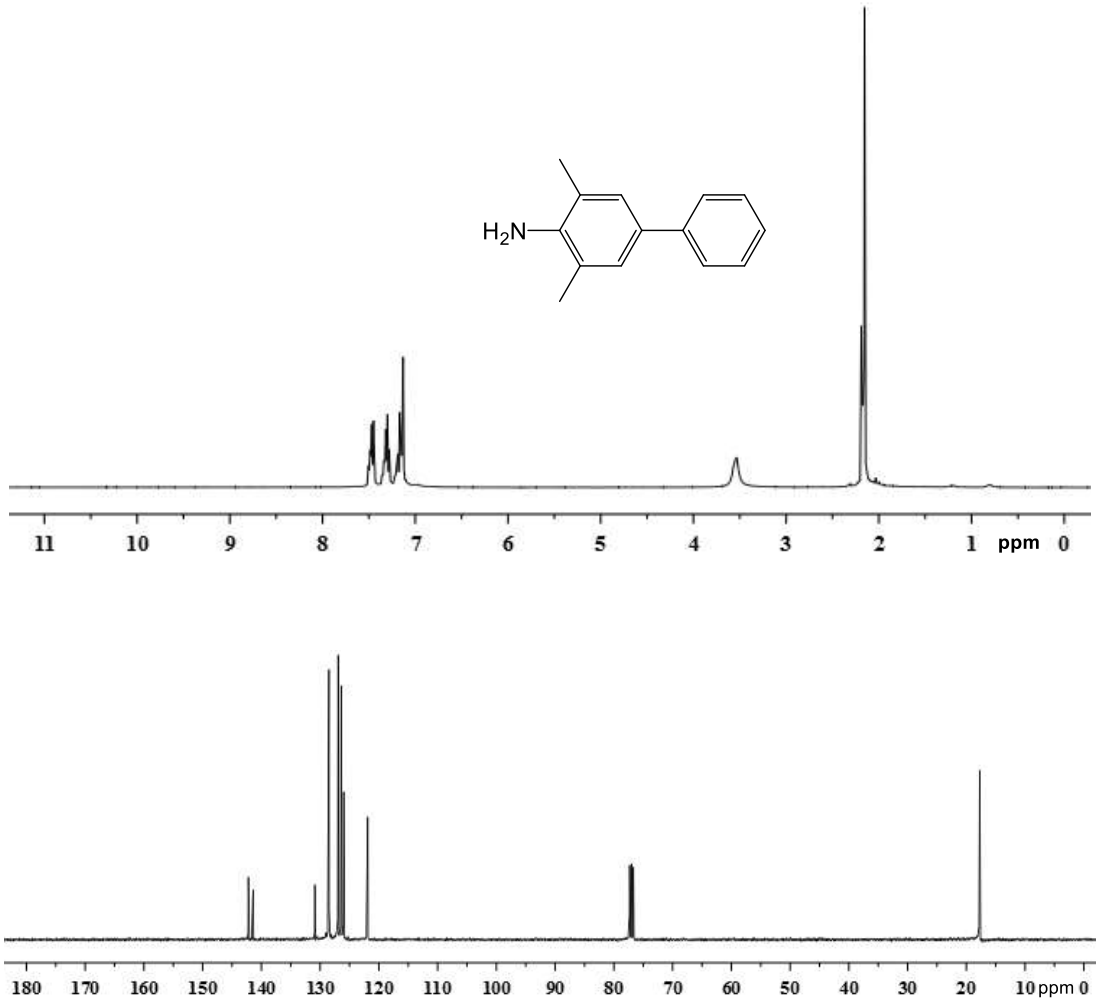

Fig. S1. ^{1}H and ^{13}C NMR spectra of 2,6-dimethyl-4-phenylaniline **1′**.

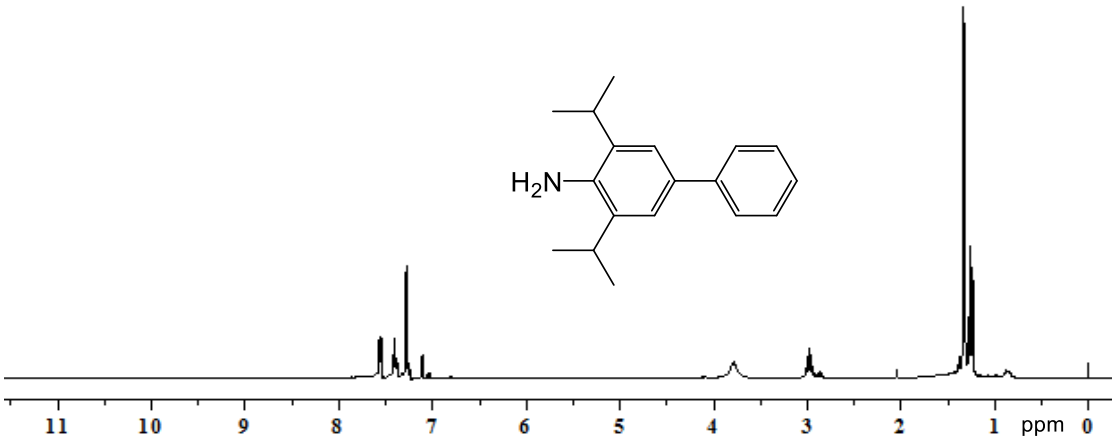

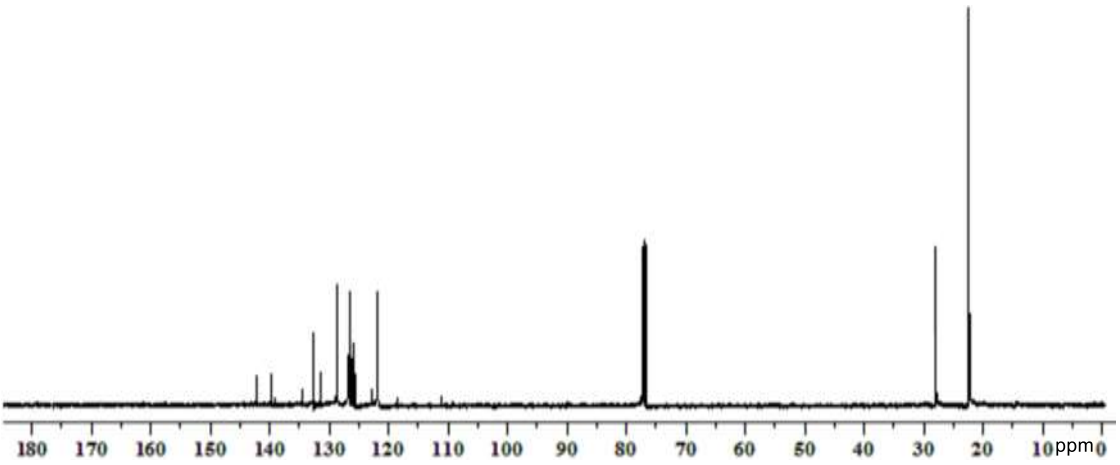

Fig. S2. ^{1}H and ^{13}C NMR spectra of 2,6-diisopropyl-4-phenylaniline **2′**.

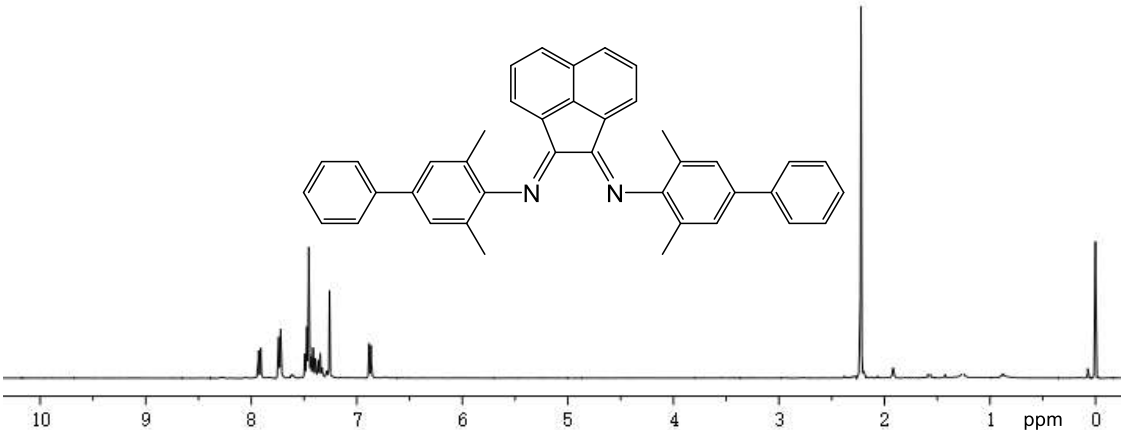

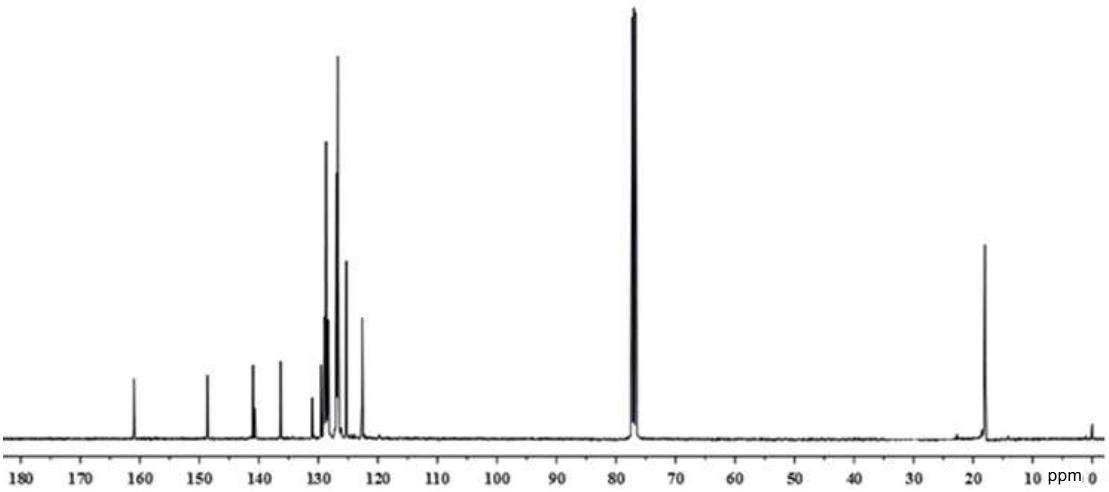

Fig. S3. ^{1}H and ^{13}C NMR spectra of ligand **L1**.

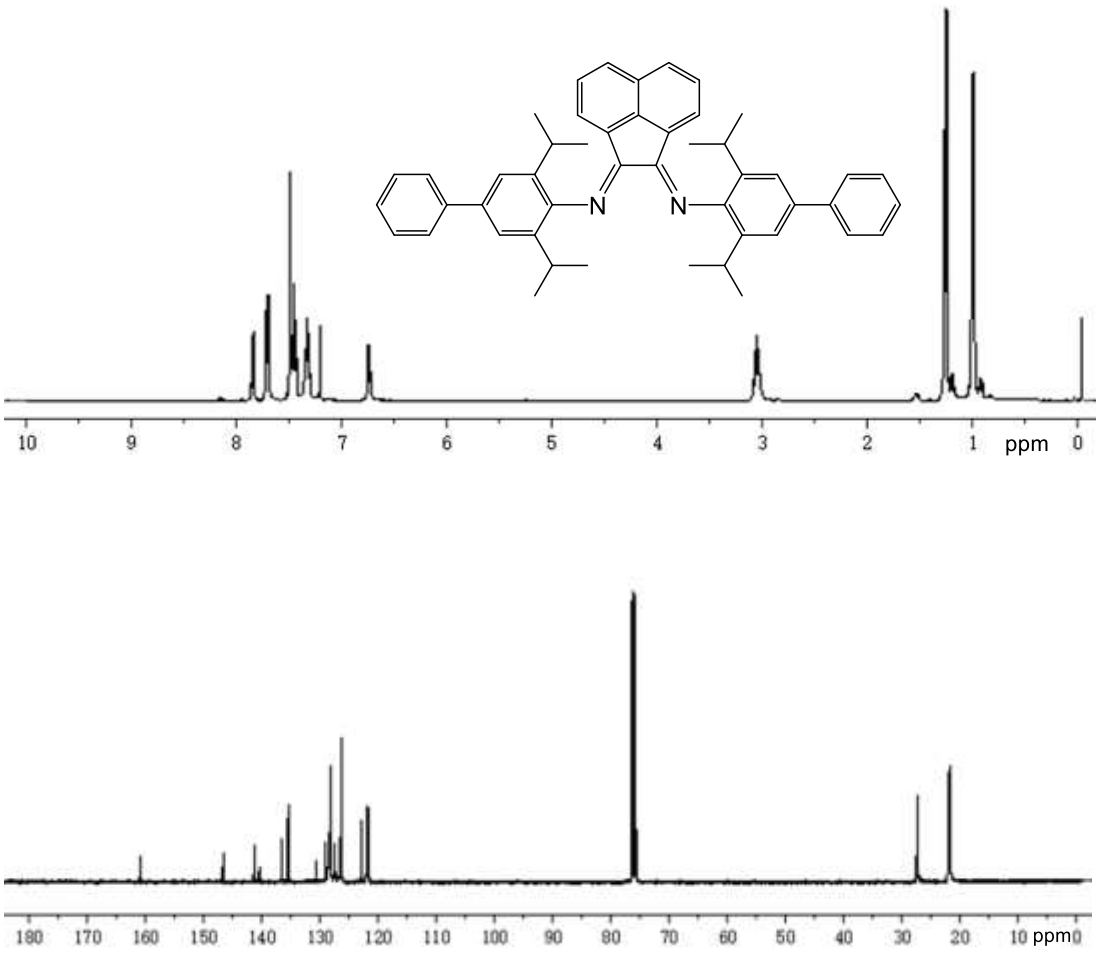

Fig. S4. ^{1}H and ^{13}C NMR spectra of ligand **L2**.

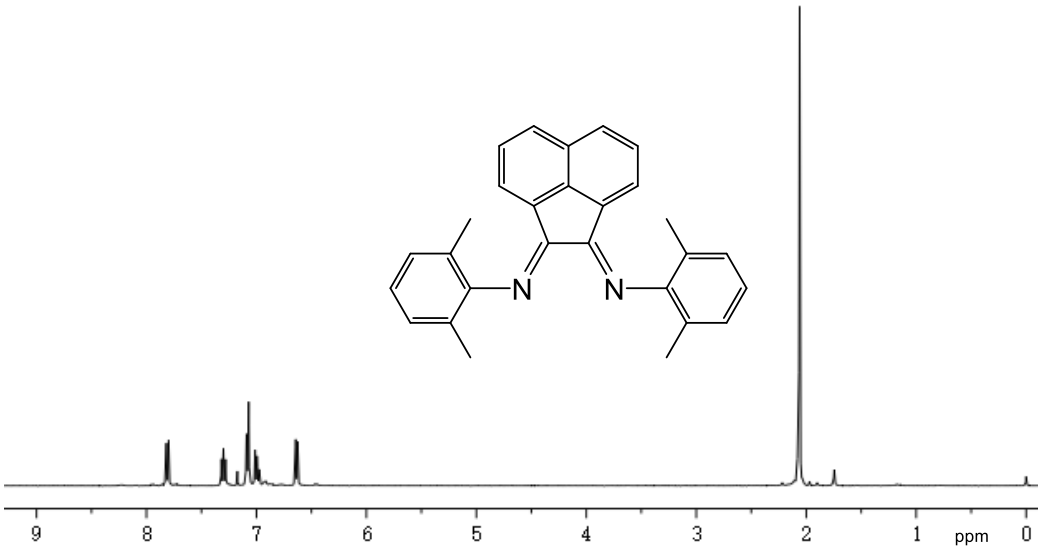

Fig. S5. ^{1}H NMR spectra of ligand **L3**.

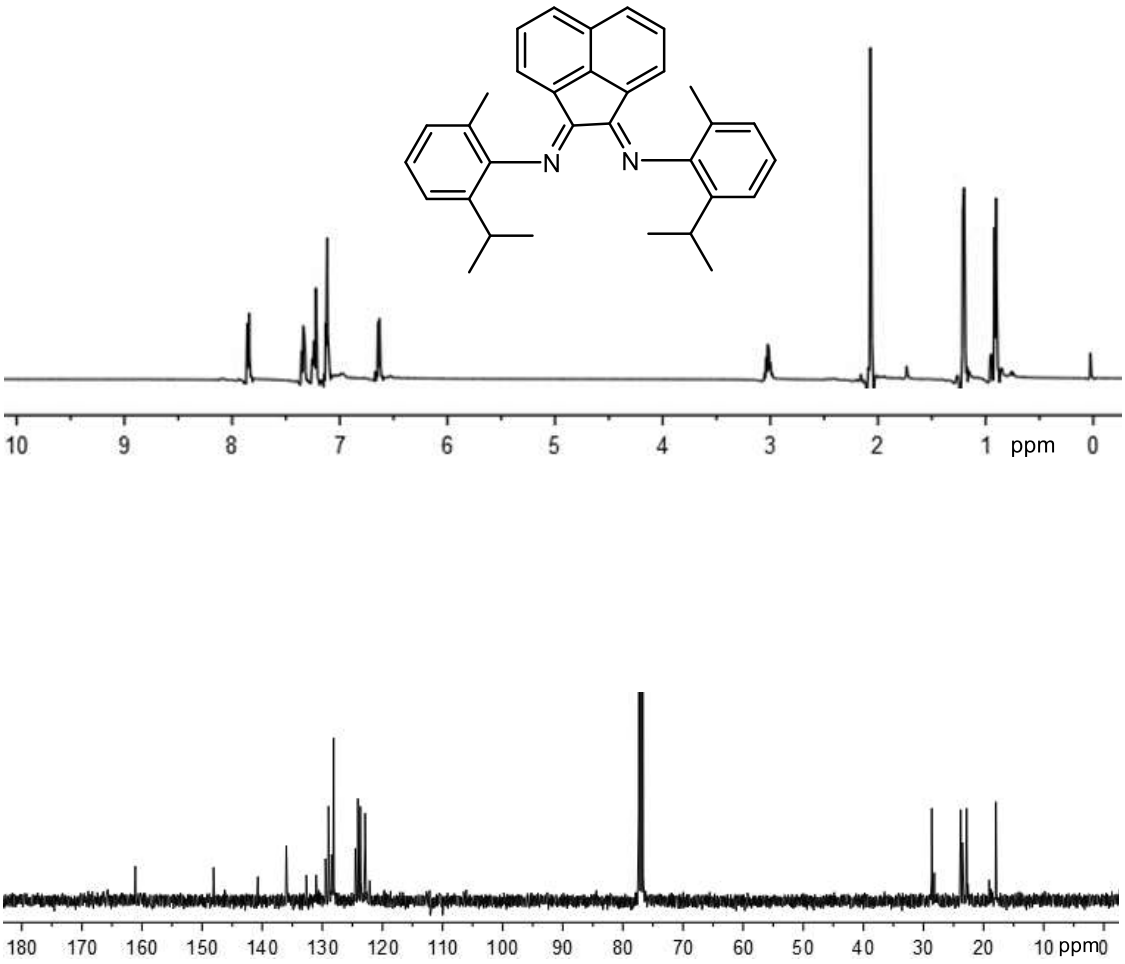

Fig. S6. ^{1}H and ^{13}C NMR spectra of ligand **L4**.

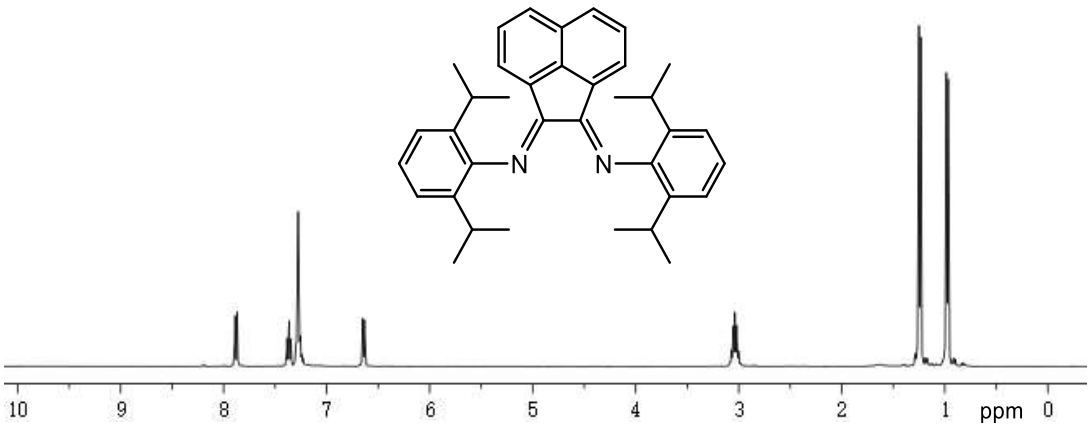

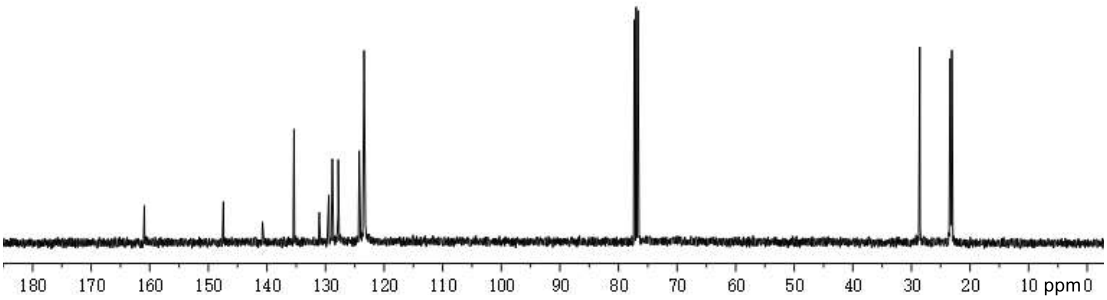

Fig. S7. ^{1}H and ^{13}C NMR spectra of ligand **L5**.

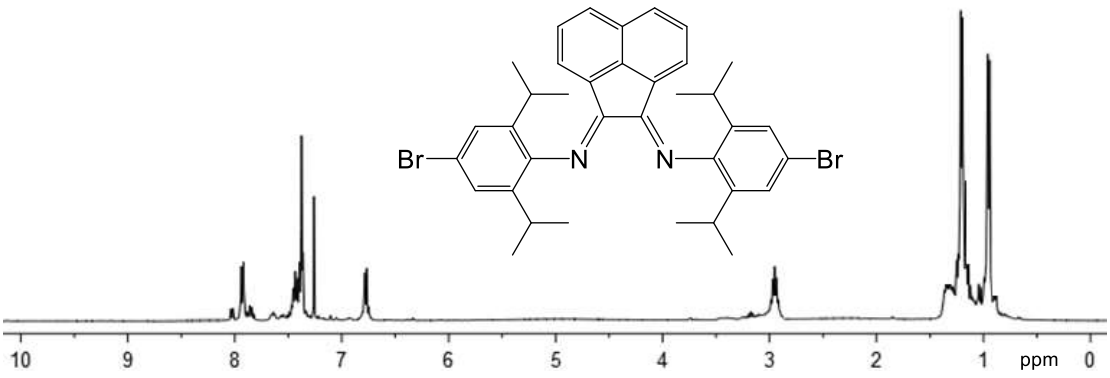

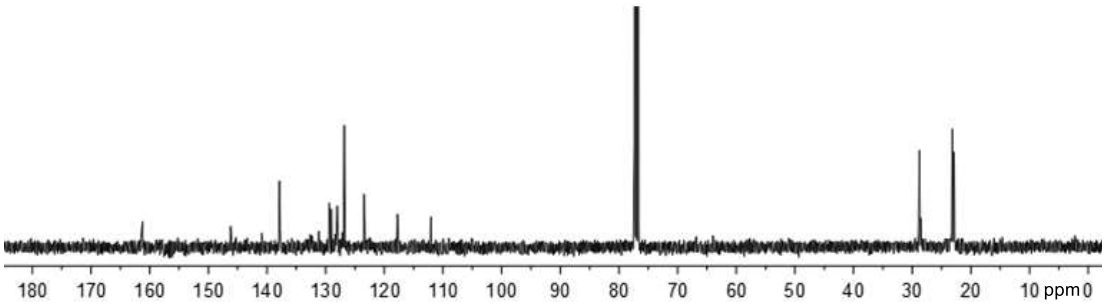

Fig. S8. ^{1}H and ^{13}C NMR spectra of ligand **L6**.

2. X-ray structure determination

The molecular structures of complexes **1** and **2** were confirmed by single-crystal X-ray diffraction in Fig. S9.

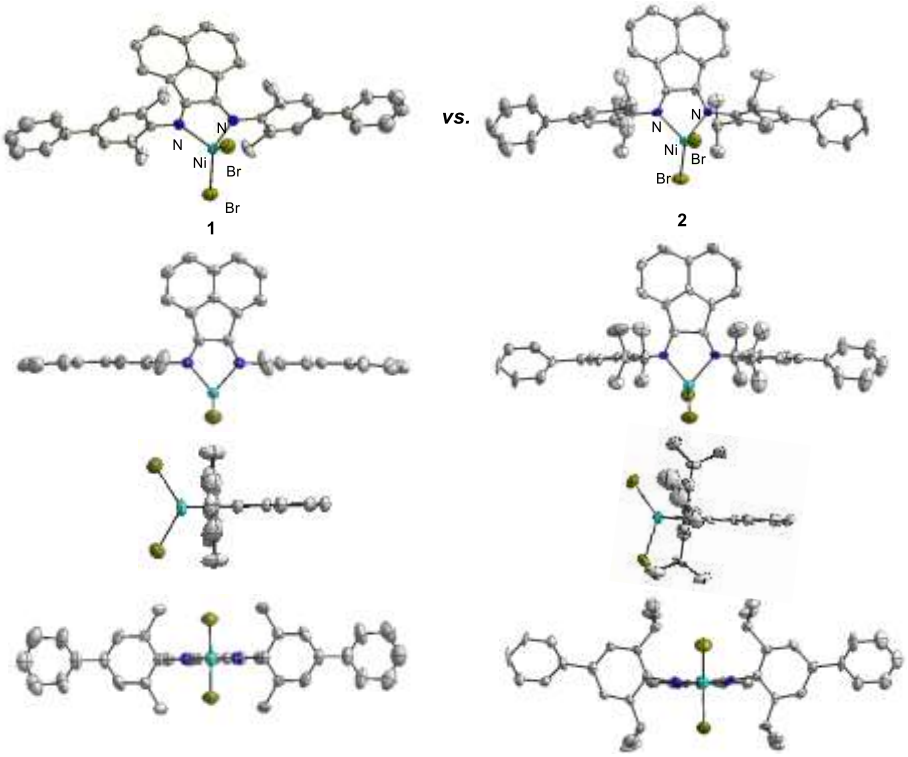

Fig. S9. Molecular structures of the catalyst precursors **1** and **2**, and H atoms have been omitted for clarity.

Table S1. Crystal data and structure refinements of **2**.

Empirical Formula	$C_{48}H_{48}Br_2N_2Ni$
Formula mass	871.41
Temperature (*K*)	296(2)
Wavelength (*Å*)	0.71073
Crystal size (mm^3)	0.22 ×0.20 ×0.19
Crystal system	Monoclinic
Space group	$P2_1/c$
a (Å)	10.934 (11)
b (Å)	21.32 (2)
c (Å)	21.40 (2)
V ($Å^3$)	4900 (8)
Z	4
Density (calcd.) (mg/cm^3)	1.181
F (000)	1792
Theta range for data collec. (°)	2.2 to 17.4
Limiting indices	$-12 \le h \le 13, -25 \le k \le 25, -25 \le l \le 21$
Reflections collected	26828

Independent reflections	8633
R_{int}	0.2083
Final R indices [$I > 2\sigma(I)$]	R_1 = 0.1425, wR_2 = 0.3145
R indices (all data)	R_1 = 0.3354, wR_2 = 0.4281
Refinement method	Full-matrix least-squares on F^2
Goodness-of-fit on F^2	1.034
Largest diff. peak and hole (e.Å^{-3})	1.936 and –0.786

3. Living/controlled polymerization of 4-octene

Polymerization of *trans*-4-octene was investigated with **1**-MMAO catalyst at 0 ℃ with the [Al]/[Ni] molar ratio of 500, and the results are summarized in Table S2.

Table S2. Living polymerization of 4-octene (4O) with **1**-MMAO at 0 ℃.[a]

Entry	Time (h)	Yield (mg)	Cov. (%)	M_n [b] (kg mol^{-1})	M_w/M_n [b]	N [c] (μmol)
1	0.25	41	8.2	11.7	1.15	3.49
2	0.50	57	11.4	16.1	1.14	3.55
3	1.00	110	22.0	28.5	1.15	3.86
4	1.50	149	29.8	38.3	1.13	3.89
5	2.00	207	41.4	53.8	1.19	3.85
6	3.00	262	52.4	67.1	1.19	3.90
7	4.00	325	65.0	83.4	1.20	3.89

[a] Polymerization conditions: Ni = 10.0 μmol; cocatalyst MMAO, [Al]/[Ni] = 500; 0.5 g of *trans*-4-octene; solvent, toluene; total volume, 5.0 mL. [b] Determined by GPC against polystyrene standard. [c] Number of polymer chains calculated by yield and M_n.

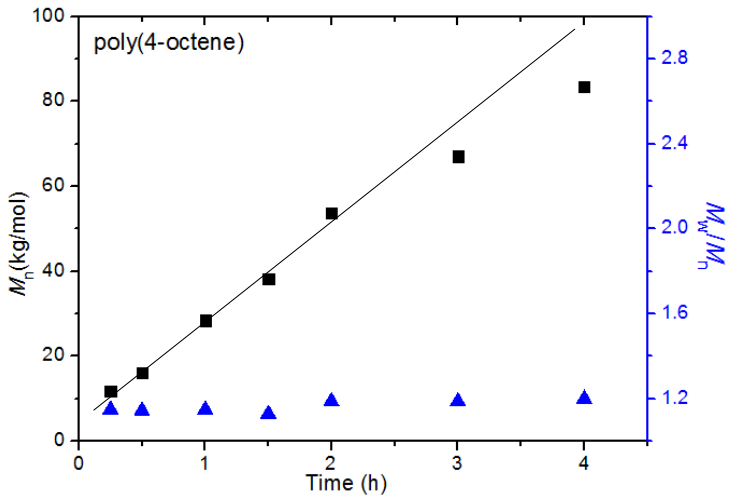

Fig. S10. Plots of M_n (■) and M_w/M_n (▲) as a function of reaction time for 4-octene polymerization catalyzed by **1**-MMAO at 0 ℃ (Table S2).

GPC curves of 4-octene polymers (Table S2):

0.25 h:

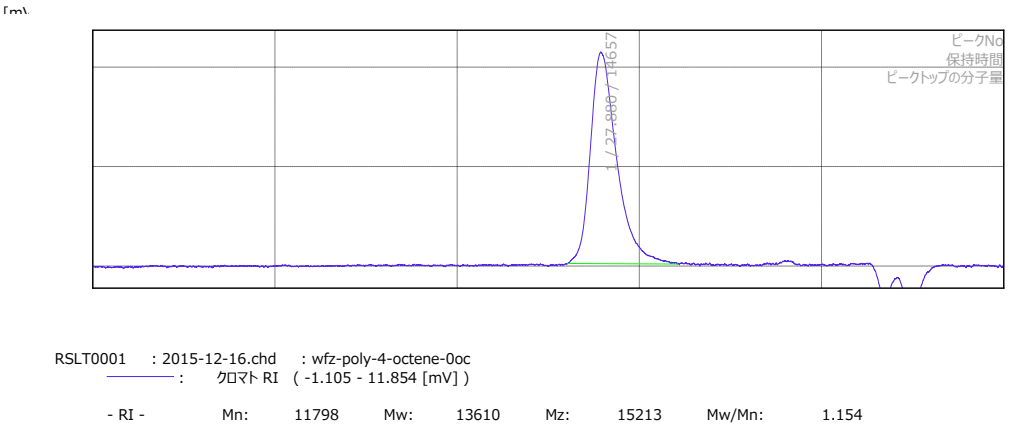

RSLT0001 : 2015-12-16.chd : wfz-poly-4-octene-0oc
: クロマト RI (-1.105 - 11.854 [mV])

- RI - Mn: 11798 Mw: 13610 Mz: 15213 Mw/Mn: 1.154

0.50 h:

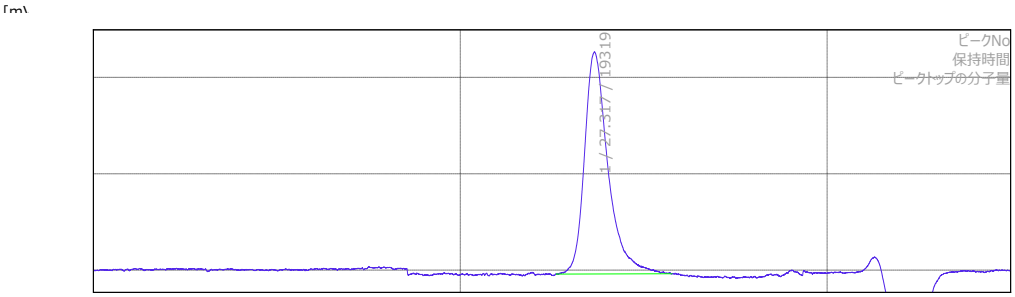

RSLT0010 : 2015-12-16.chd : wfz-poly
: クロマト RI (-1.145 - 12.464 [mV])

- RI - Mn: 16070 Mw: 18385 Mz: 20386 Mw/Mn: 1.144

1.00 h:

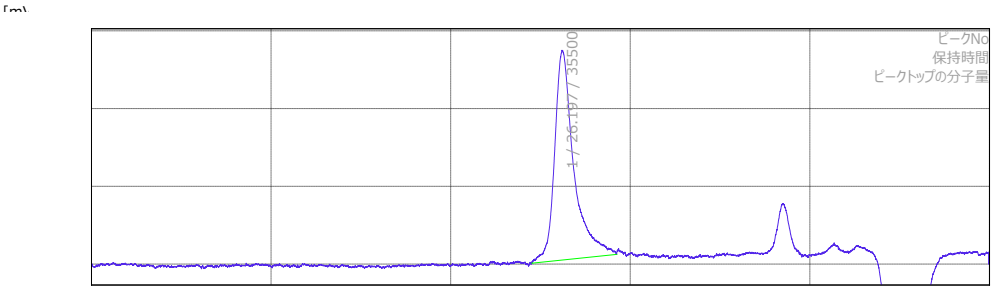

RSLT0006 : 2015-08-04.chd : wang-no-71-2
: クロマト RI (-0.536 - 6.051 [mV])

- RI - Mn: 28453 Mw: 32683 Mz: 36339 Mw/Mn: 1.149

1.50 h:

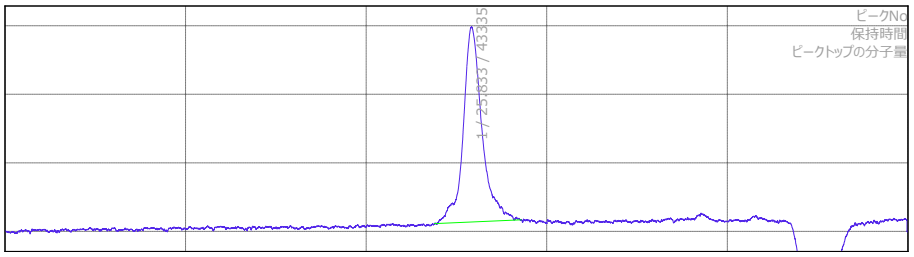

RSLT0008 : 2015-08-02.chd : wang-no-67-4
: クロマト RI (-0.580 - 6.573 [mV])

- RI - Mn: 38299 Mw: 43107 Mz: 48260 Mw/Mn: 1.126

2.00 h:

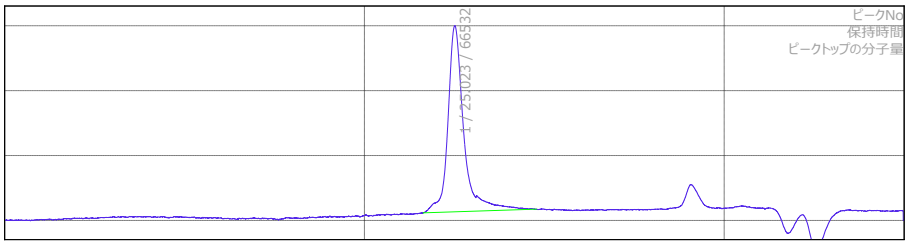

RSLT0011 : 2015-12-11.chd : wfz-poly-4-octene-0oc
: クロマト RI (-1.472 - 16.517 [mV])

- RI - Mn: 53798 Mw: 63892 Mz: 71304 Mw/Mn: 1.188

3.00 h:

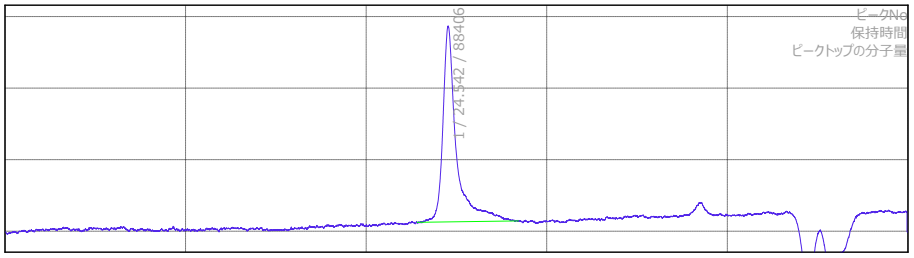

RSLT0004 : 2015-01-07.chd : wfz-4o
: クロマト RI (-0.581 - 6.317 [mV])

- RI - Mn: 67103 Mw: 79797 Mz: 88125 Mw/Mn: 1.189

4.00 h:

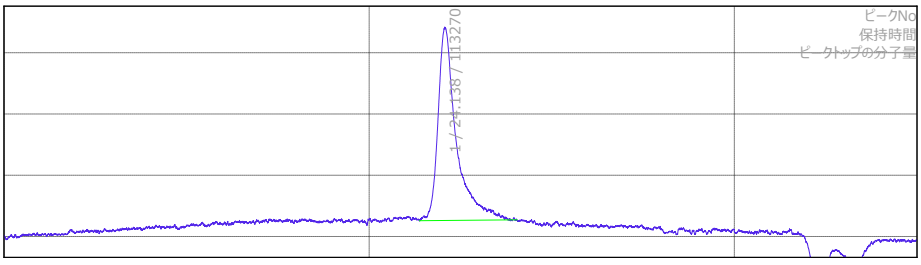

RSLT0008 : 2015-02-03.chd : wfz-entry2
: クロマト RI (-0.678 - 7.518 [mV])

- RI - Mn: 83448 Mw: 100098 Mz: 111841 Mw/Mn: 1.200

Fig. S11. GPC traces for the poly(4-octene)s obtained with **1**-MMAO at 0 °C for 0.25–4.00 h (entries 1−7, Table S2).

4. Equations for the microstructure analysis of the polymers

Calculation of the degree of branching

The degree of branching was estimated by ^{1}H NMR spectroscopy and was corrected for end groups as follows [3]:

$$B = \frac{2(I_{CH_3})}{3(I_{CH} + I_{CH_2} + I_{CH_3})} \times 1000 \qquad \text{(Eq. S1)}$$

Where B refers to branching degree (the number of methyl carbon in every 1000 carbons), and CH_3, CH_2, CH refer to the intensities of the methyl, methylene and methane resonances in ^{1}H NMR spectra.

Calculation of the contents of the total CH_3 and each branch

The ^{13}C NMR spectra of the poly(2-octene) confirm the presence of methyl (19.92 ppm, $1B_1$), ethyl (11.08 ppm, $1B_2$), amyl (32.60 ppm, $3B_5$), hexyl (31.99 ppm, $3B_6$) branches, whereas those of poly(4-octene) showed the resonances of propyl (14.76 ppm, $1B_3$) and butyl (14.38 ppm, $1B_4$) branches. Poly(1-octene) showed the resonances of methyl (19.76 ppm, $1B_1$) and hexyl (14.18 ppm, $1B_6$) branches. By the use of these resonances of the branching carbans, i.e., $1B_1$, $1B_2$, $1B_3$, $1B_4$, $1B_5$, $1B_6$, $2B_3$, $2B_4$ and $3B_6$, the contents of the total CH_3 and each branch can be determined by the following equation [3]:

$$\mathbf{CH_3} = I_{1B_1} + I_{1B_2} + \left(I_{1B_3} + I_{3B_3}\right)/2 + I_{1B_4} + I_{1B_5} + I_{1B_6}$$

Methyl branch, $\mathbf{Me} = I_{1B_1} + I_{2B_3} - I_{1B_3}$; Ethyl branch, $\mathbf{Et} = \left(I_{1B_2} + I_{2B_2}\right)/2$

Propyl branch, $\mathbf{Pr} = \left(I_{1B_3} + I_{3B_3}\right)/2$; Butyl branch, $\mathbf{Bu} = \left(I_{1B_4} + I_{2B_4}\right)/2$

Amyl branch, $\mathbf{Amy} = I_{1B_5} + I_{1B_6} - I_{3B_6}$; Hexyl branch, $\mathbf{He} = I_{3B_6}$ (Eq. S2)

Where branching numbers per 1000 carbon atoms were determined by ^{13}C NMR.

Calculation of 1,8-enchainment of 1-octene

The fraction of 1,8-enchainment was calculated using the following equation S3 [3]:

$$1,8\text{-}\% = \frac{1000 - 6B}{1000 + 2B} \times 100 \qquad \text{(Eq. S3)}$$

Where B is the total branching calculated by Eq. S1.

Calculation of 1,8-enchainment of 1-octene in octane isomer copolymer

The fraction of 1,8-enchainment was calculated using the following equation S4 [3]:

$$1,8\text{-}\% = \frac{1000 - B}{125} \times 100 \qquad \text{(Eq. S4)}$$

where B is the total branching calculated by Eq. S1.

Calculation of 1-octene and 4-octene in the poly(1O-co-4O)

The content of 1- and 4-octenes of the poly(1O-*co*-4O) was calculated as follows:

$$[4O] = [Pr]+[Bu] = (I_{1B_3}+I_{3B_3})/2 + (I_{1B_4}+I_{2B_4})/2 \quad \text{(Eq. S5)}$$

$$[1O] = 1 - [4O]$$

where [1O] and [4O] is the content of 1-octene and 4-octene of the poly(1O-*co*-4O), respectively. [Pr] and [Bu] were determined by ^{13}C NMR and calculated by Eq. S2.

5. ^{1}H and ^{13}C NMR spectra of polymers and copolymers

5.1. ^{1}H and ^{13}C NMR spectra of poly(4-octene)s

P4O:

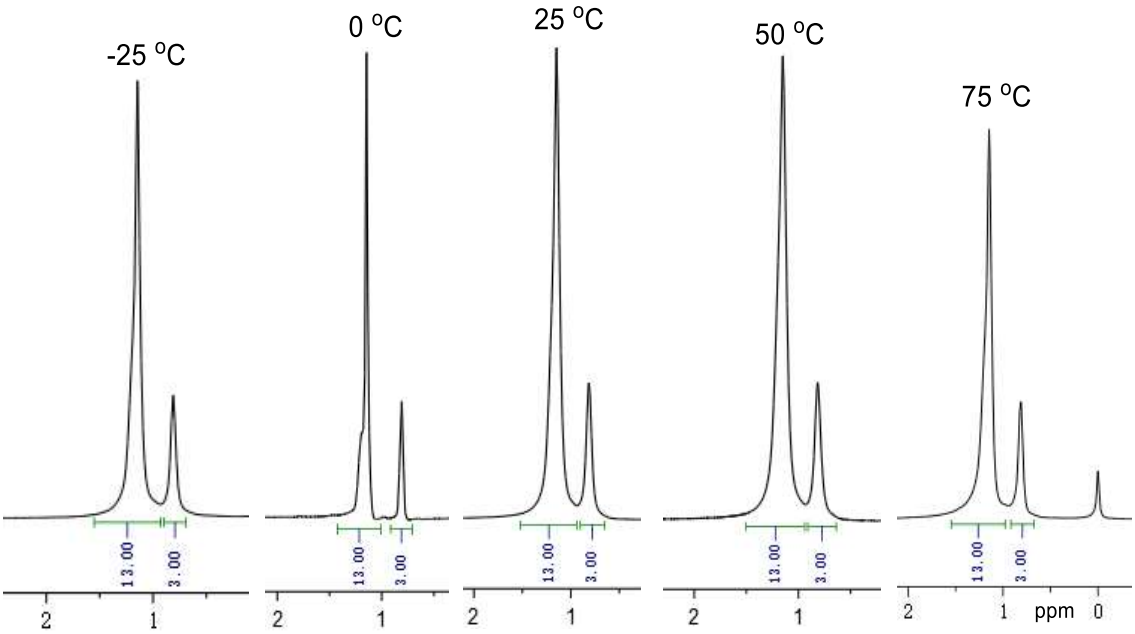

Fig. S12. ^{1}H NMR spectra of the poly(4-octene)s obtained by **1**-MMAO at different temperatures (entries 1−5, Table 2).

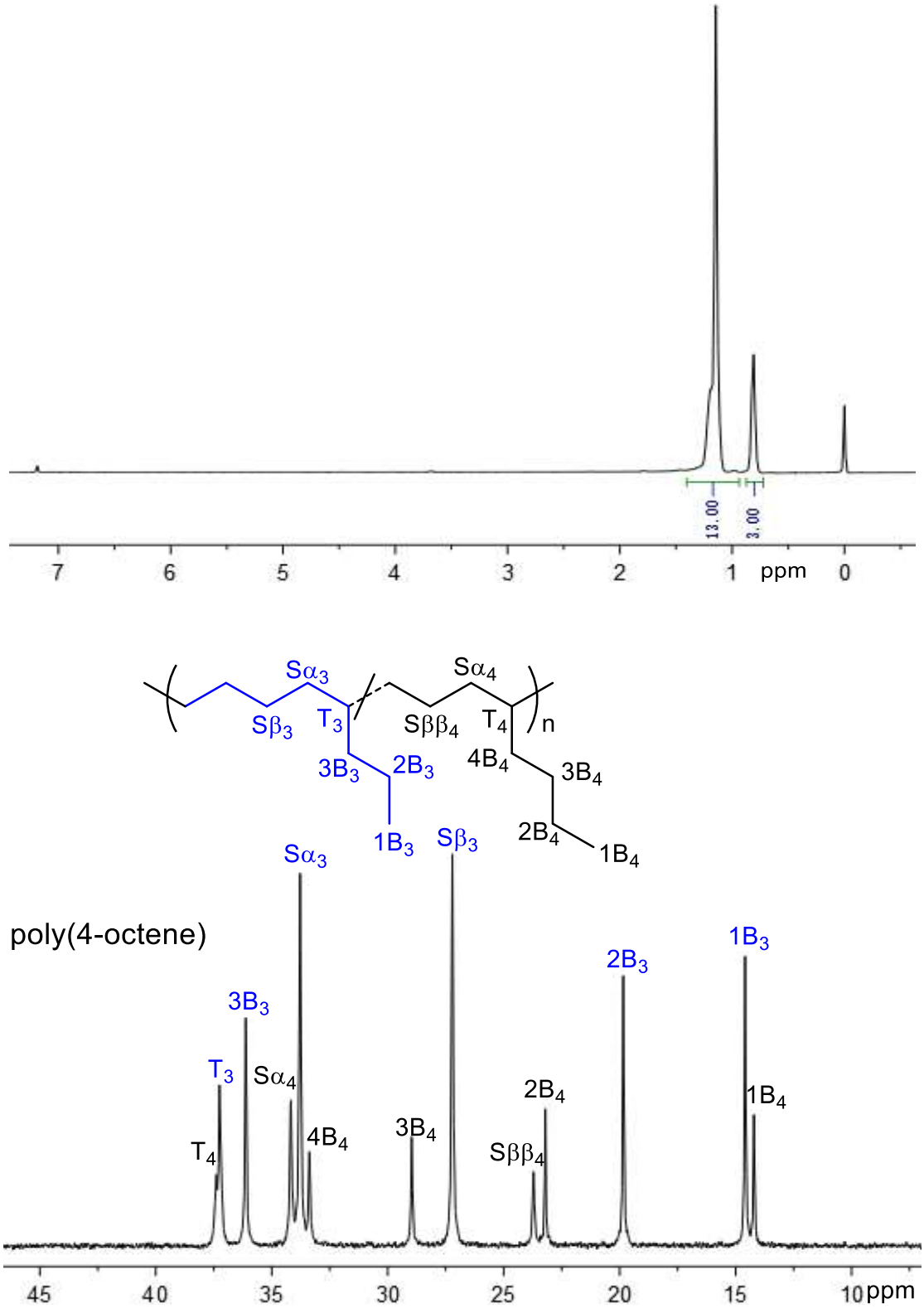

Fig. S13. ^{1}H and ^{13}C NMR spectra of poly(4-octene) obtained with **5**-MMAO at 20 ^{o}C for 2 h (entry 7, Table 1).

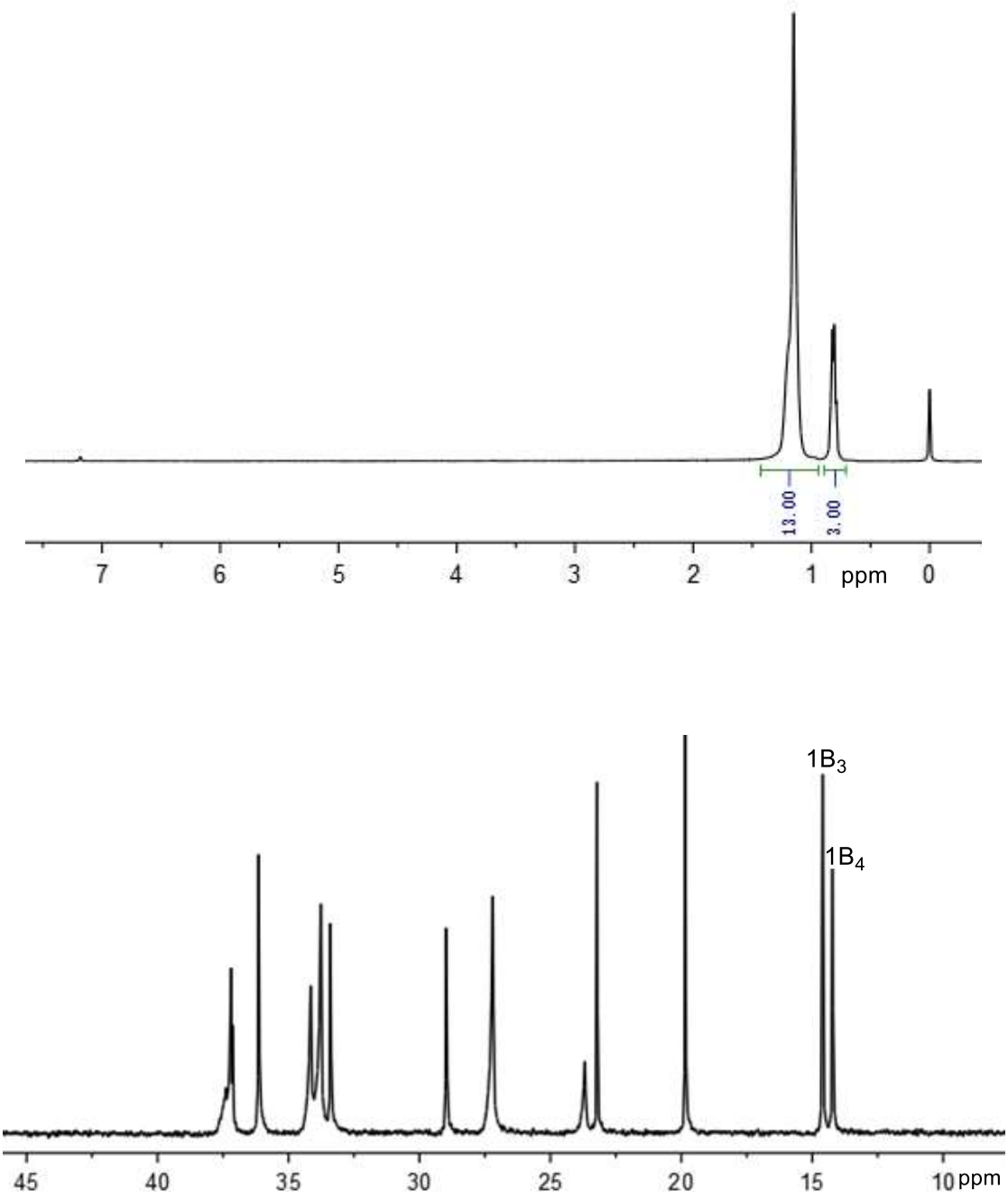

Fig. S14. ^{1}H and ^{13}C NMR spectra of poly(4-octene) obtained with **3**-MMAO at 20 ^{o}C for 2 h (entry 5, Table 1).

5.2. ^{1}H and ^{13}C NMR spectra of poly(2-octene)s

P2O:

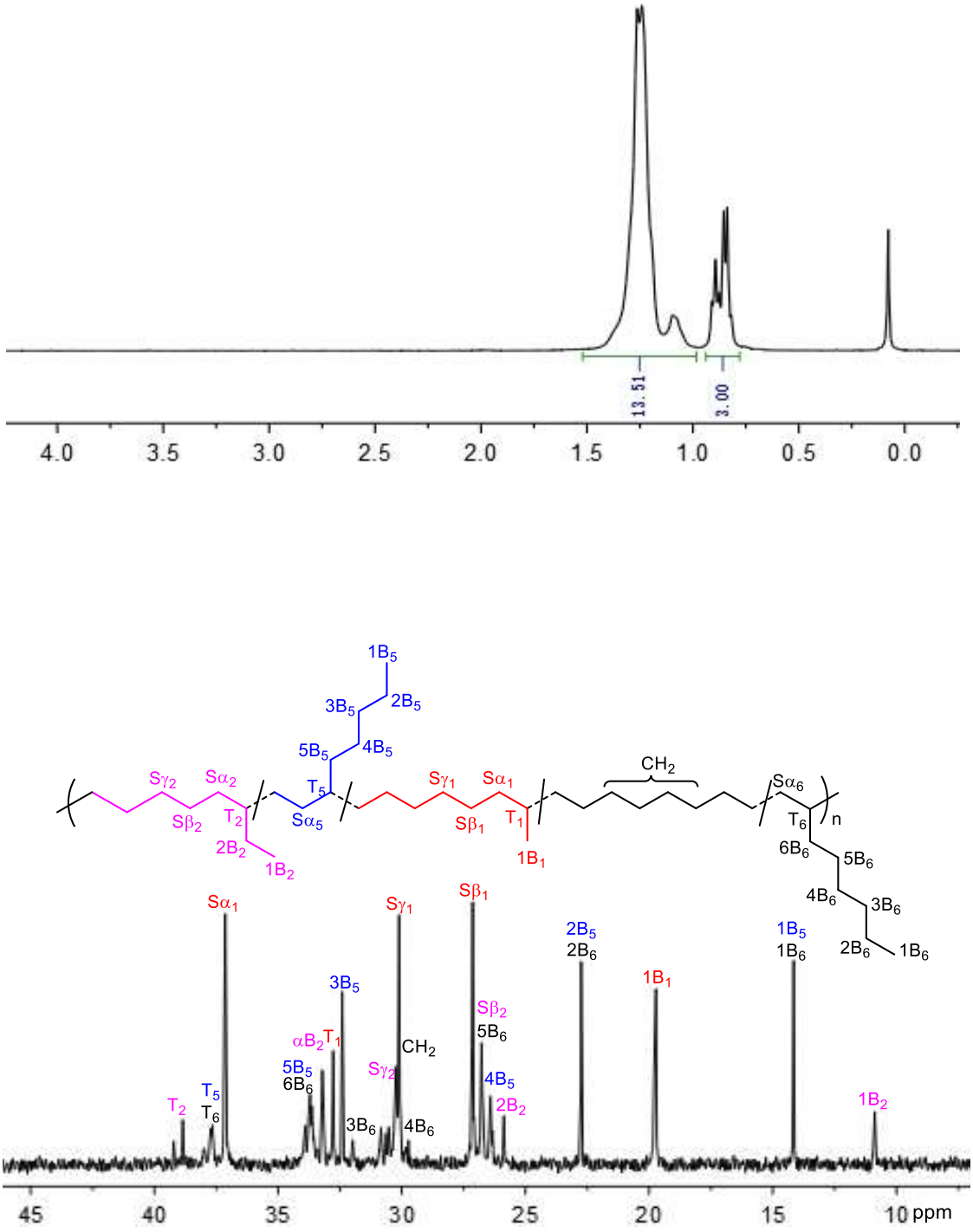

Fig. S15. ^{1}H and ^{13}C NMR spectra of poly(2-octene) obtained with **1**-MMAO at 0 ^{o}C for 2 h (entry 12, Table 2).

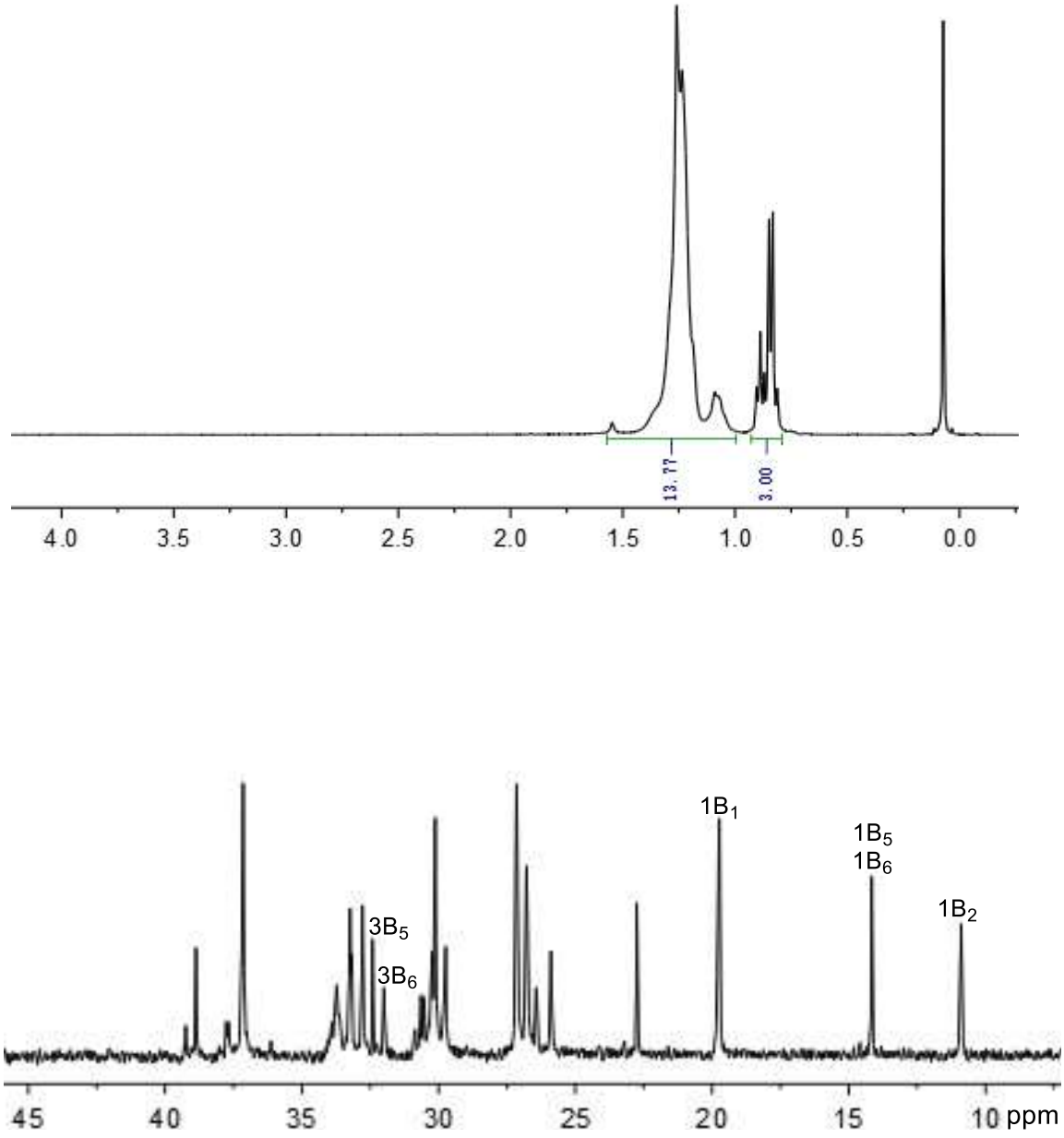

Fig. S16. ^{1}H and ^{13}C NMR spectra of poly(2-octene) obtained with **1**-MMAO at 25 ^{o}C for 2 h (entry 13, Table 2).

5.3. ^{1}H and ^{13}C NMR spectra of poly(1-octene)s

P1O:

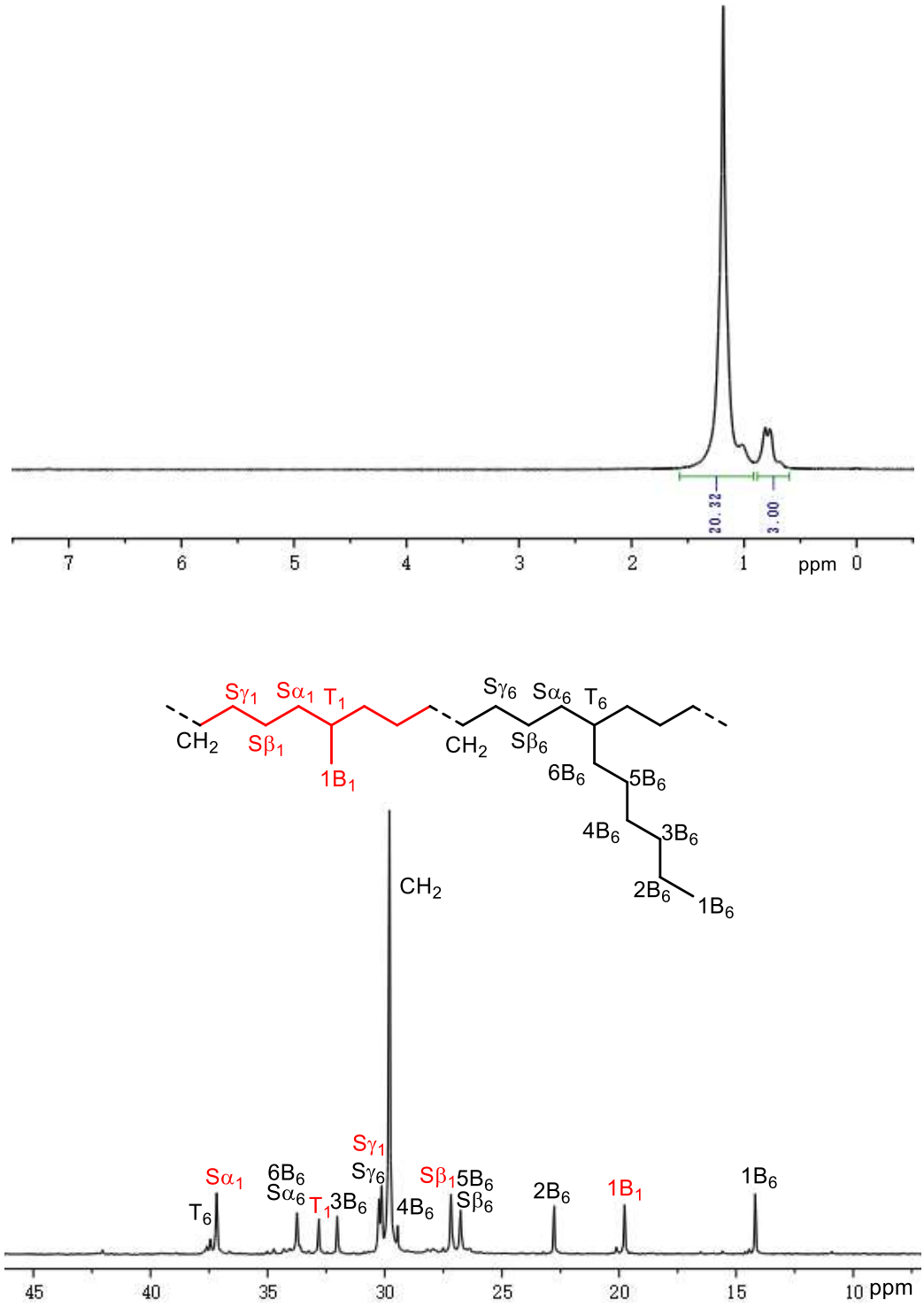

Fig. S17. ^{1}H and ^{13}C NMR spectra of poly(1-octene) obtained with **1**-MMAO at 25 °C for 2 h (entry 15, Table 2).

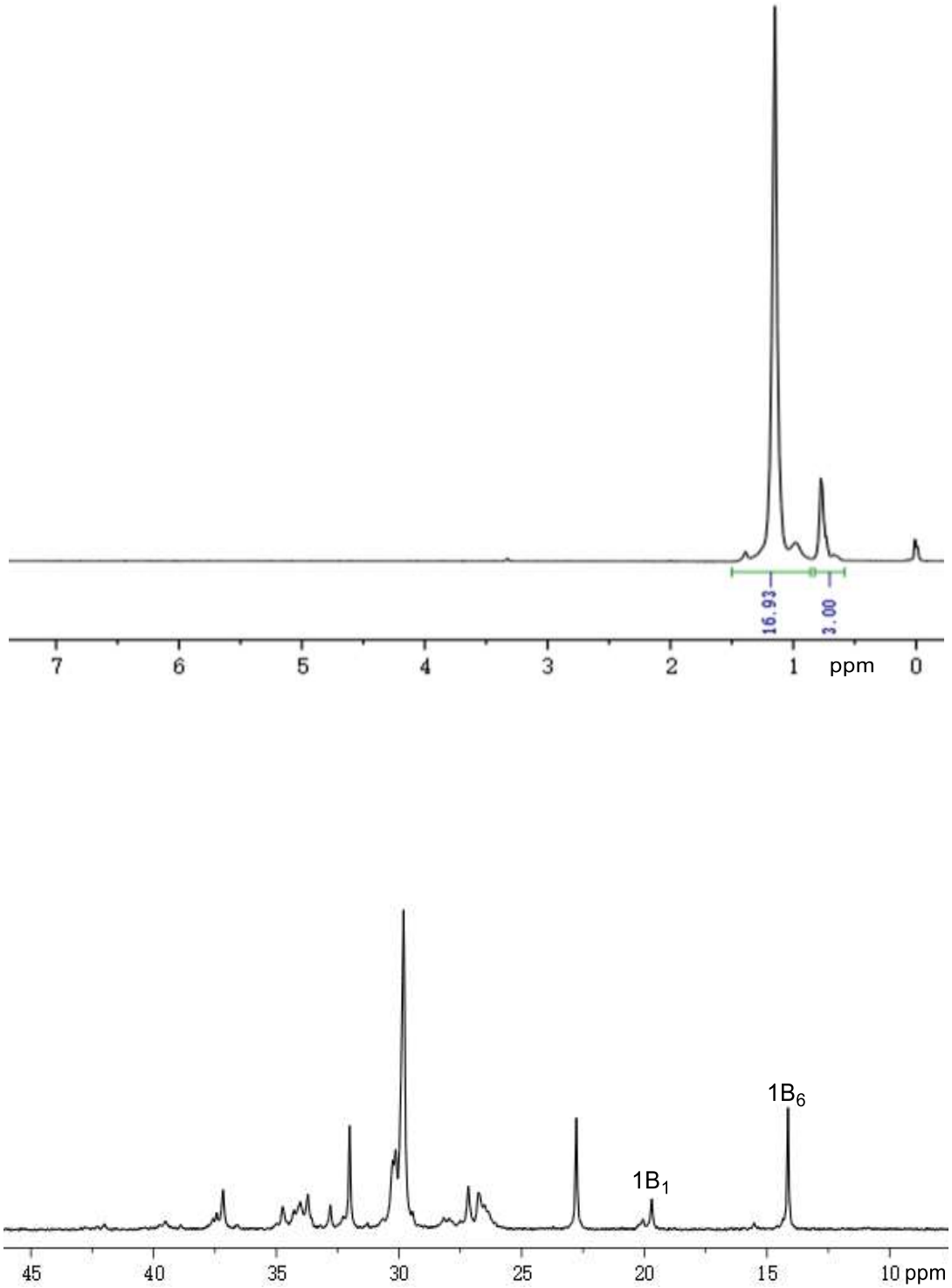

Fig. S18. ^{1}H and ^{13}C NMR spectra of poly(1-octene) obtained with **1**-MMAO at 0 ^{o}C for 2 h (entry 14, Table 2).

5.4. ^{1}H and ^{13}C NMR spectra of 1-octene with 2-, 3- and 4-octene copolymers

Poly(1O-*co*-4O):

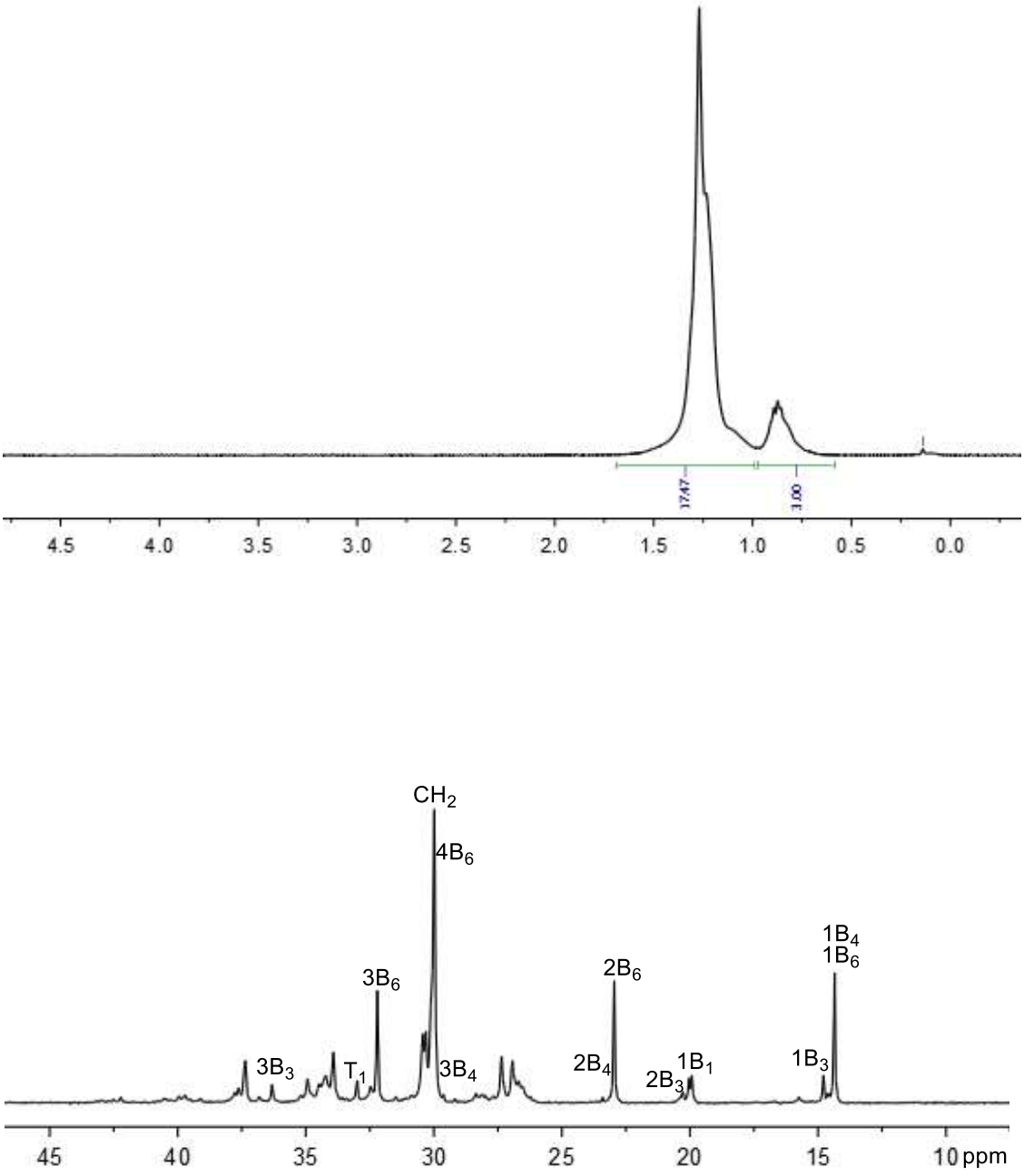

Fig. S19. ^{1}H and ^{13}C NMR spectra of 1O-4O copolymer obtained with **1**-MMAO at 0 ^{o}C for 2 h (entry 1, Table 3).

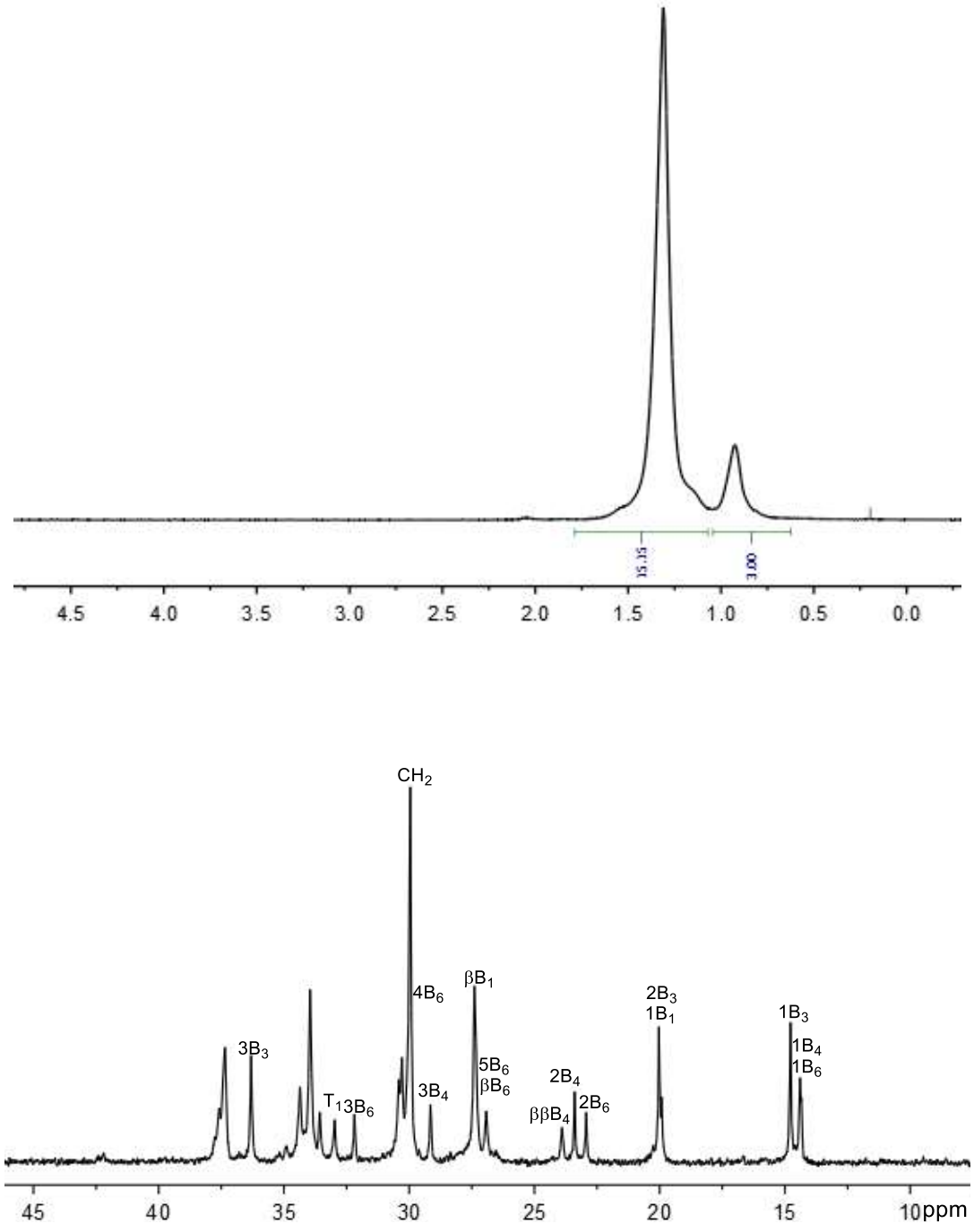

Fig. S20. ^{1}H and ^{13}C NMR spectra of 1O-4O copolymer obtained with **1**-MMAO at 25 ^{o}C for 2 h (entry 2, Table 3).

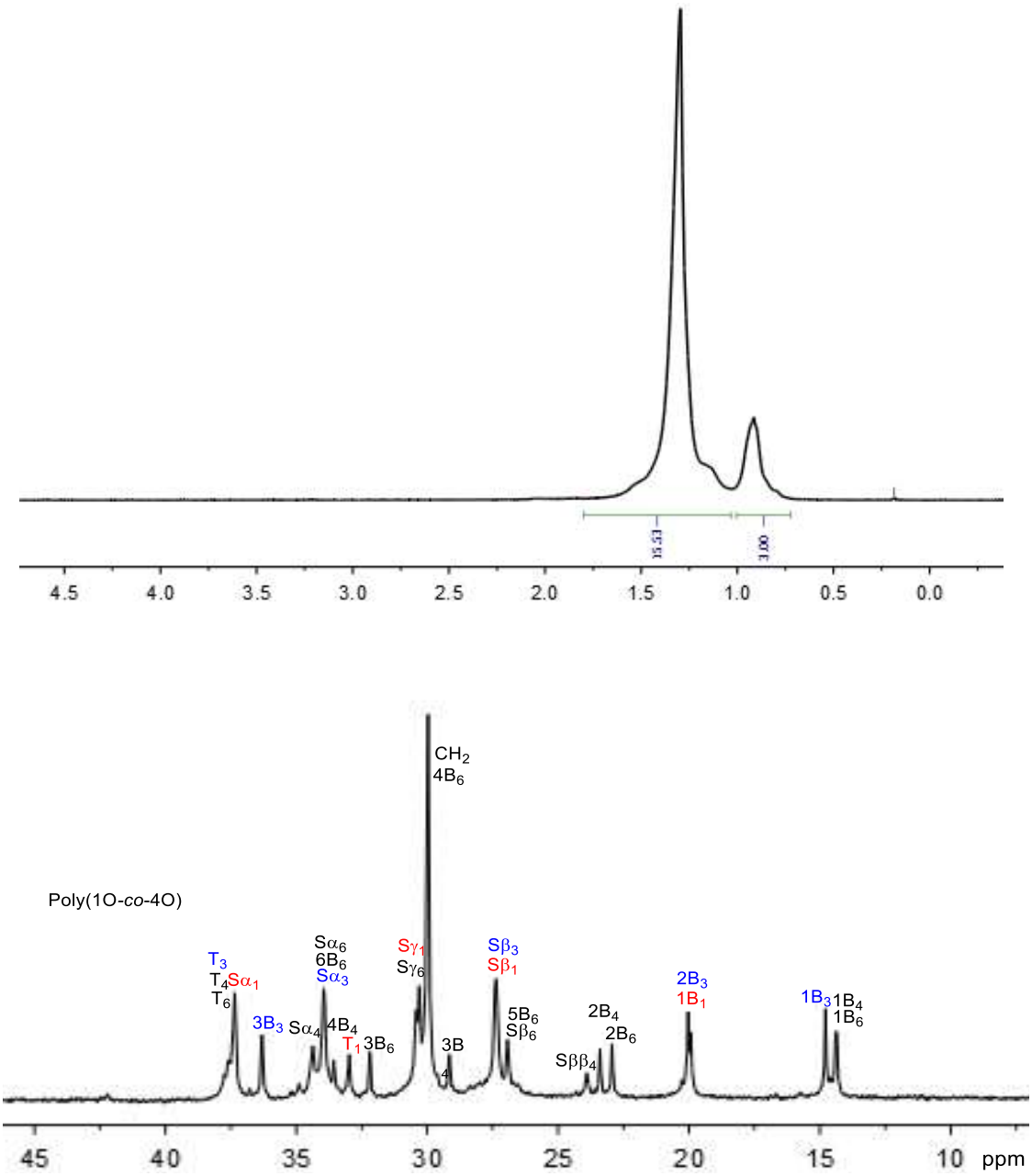

Fig. S21. ^{1}H and ^{13}C NMR spectra of 1O-4O copolymer obtained with **2**-MMAO at 25 ^{o}C for 2 h (entry 3, Table 3).

Poly(1O-*co*-3O):

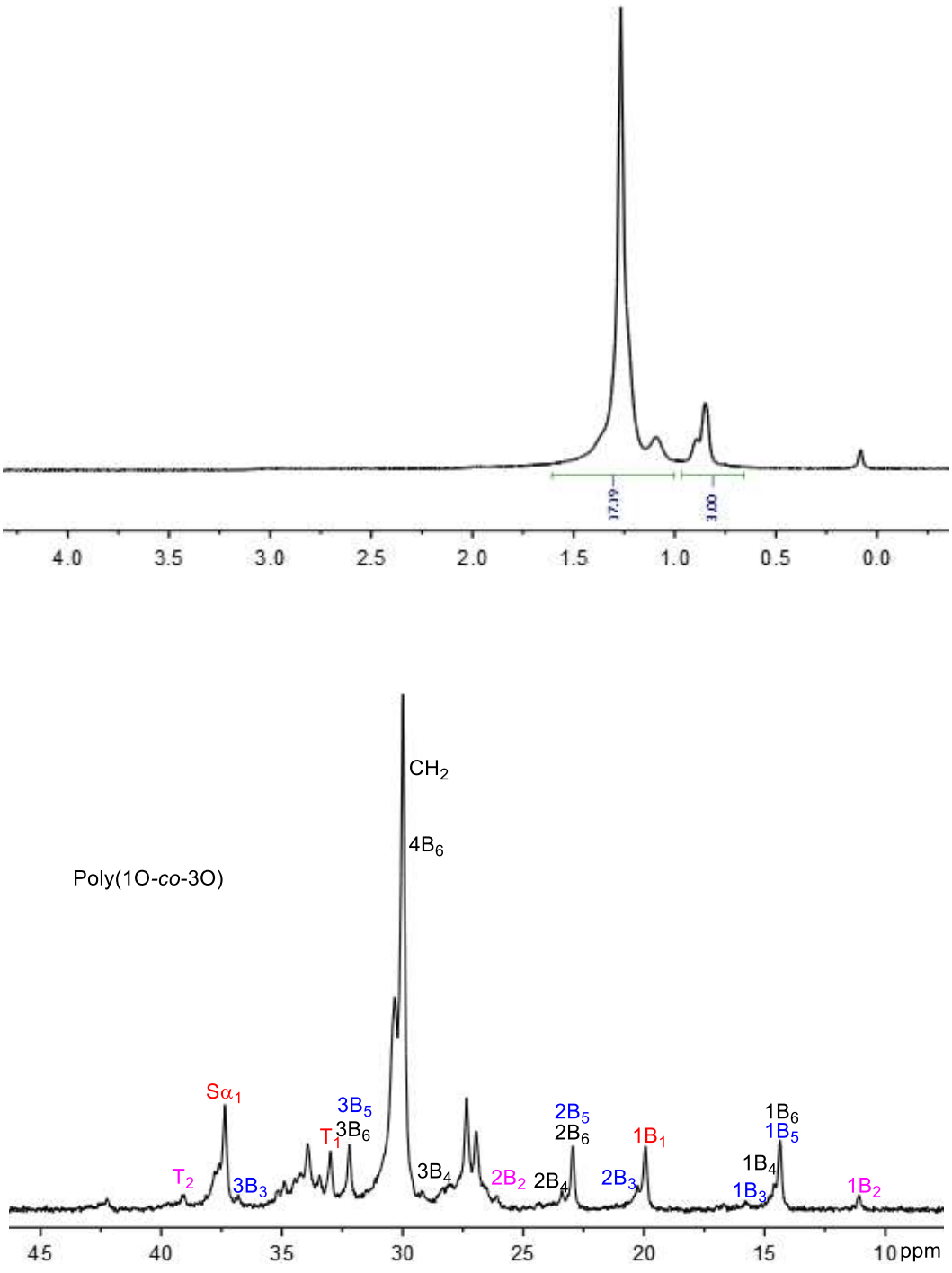

Fig. S22. [1] H and [13]C NMR spectra of 1O-3O copolymer obtained with **1**-MMAO at 25 [o]C for 2 h (entry 4, Table 3).

Poly(1O-*co*-2O):

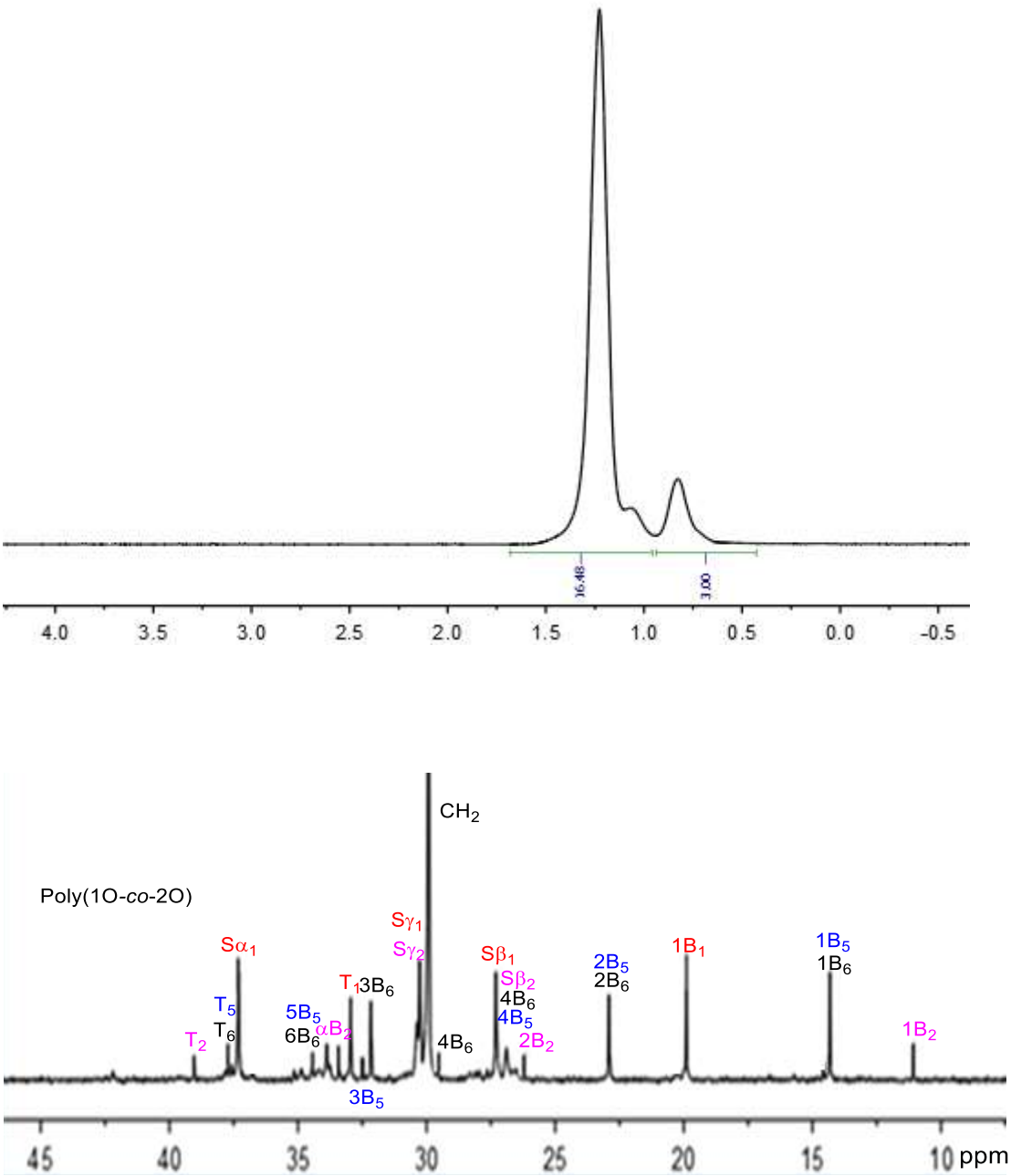

Fig. S23. ^{1}H and ^{13}C NMR spectra of 1O-2O copolymer obtained with **1**-MMAO at 25 ^{o}C for 2 h (entry 5, Table 3).

6. GPC curves of polymers and copolymers

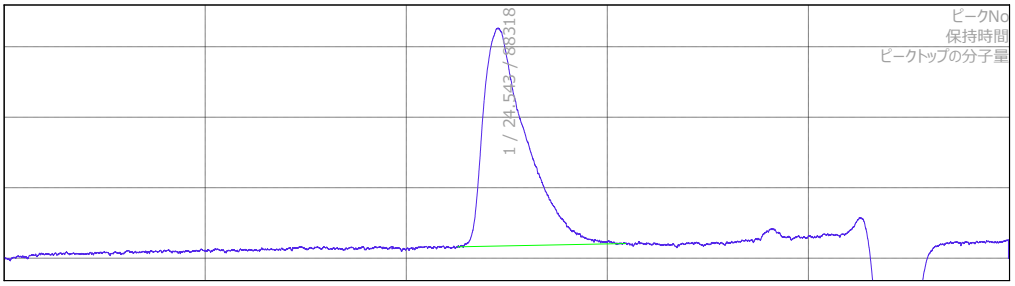

RSLT0006 : 2015-12-15(2).chd : wfz-poly-4-octene
: クロマト RI (-0.632 - 7.183 [mV])

- RI - Mn: 46690 Mw: 72468 Mz: 94815 Mw/Mn: 1.552

Fig. S24. GPC trace of the poly(4-octene) obtained with **1**-MMAO at 20 ℃ for 2 h (entry 2, Table 1).

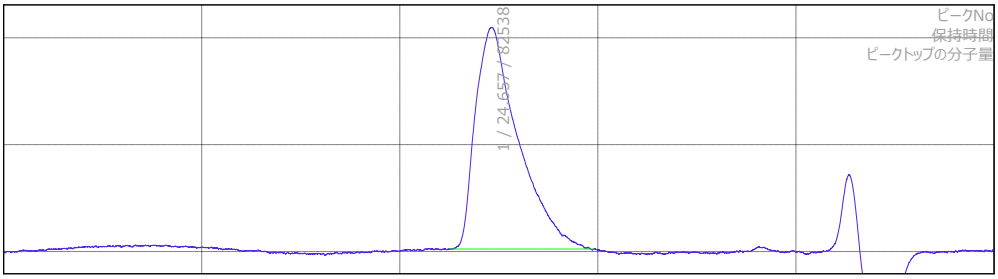

RSLT0007 : 2015-12-15(2).chd : wfz-poly-4-octene-0oc-7
: クロマト RI (-1.034 - 11.538 [mV])

- RI - Mn: 49029 Mw: 74433 Mz: 98094 Mw/Mn: 1.518

Fig. S25. GPC trace of the poly(4-octene) obtained with **2**-MMAO at 20 ℃ for 2 h (entry 4, Table 1).

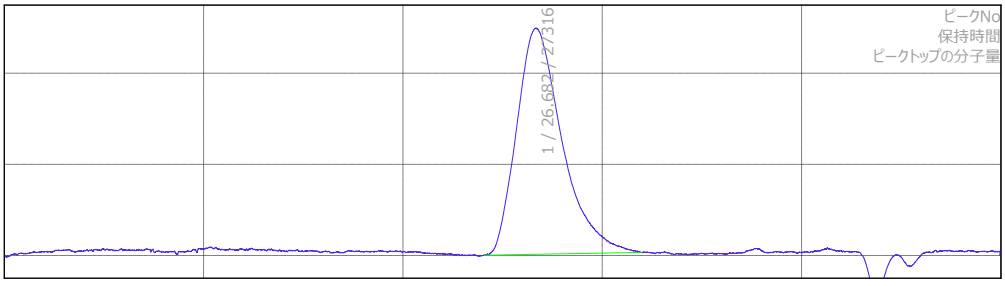

RSLT0002 : 2015-07-18.chd : wang-no-54-2-octene-rt.-c1
: クロマト RI (-1.235 - 13.728 [mV])

- RI - Mn: 18671 Mw: 27067 Mz: 35460 Mw/Mn: 1.450

Fig. S26. GPC trace of the poly(4-octene) obtained with **3**-MMAO at 20 ℃ for 2 h (entry 5, Table 1).

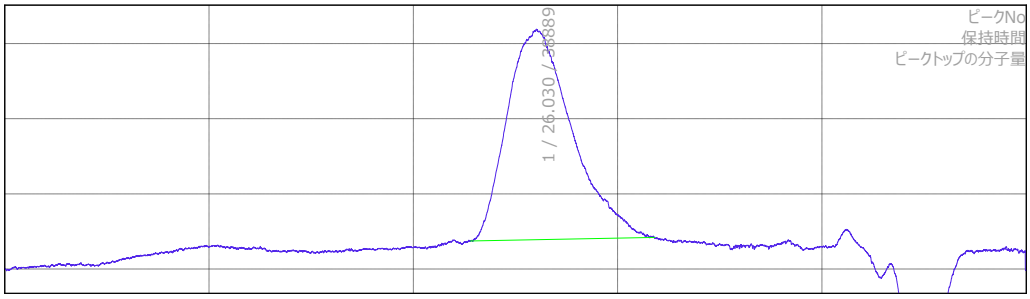

RSLT0003 : 2015-08-04.chd : wang-no-72
: クロマト RI (-0.644 - 7.023 [mV])

- RI - Mn: 22939 Mw: 43427 Mz: 68214 Mw/Mn: 1.893

Fig. S27. GPC trace of the poly(4-octene) obtained with **4**-MMAO at 20 ℃ for 2 h (entry 6, Table 1).

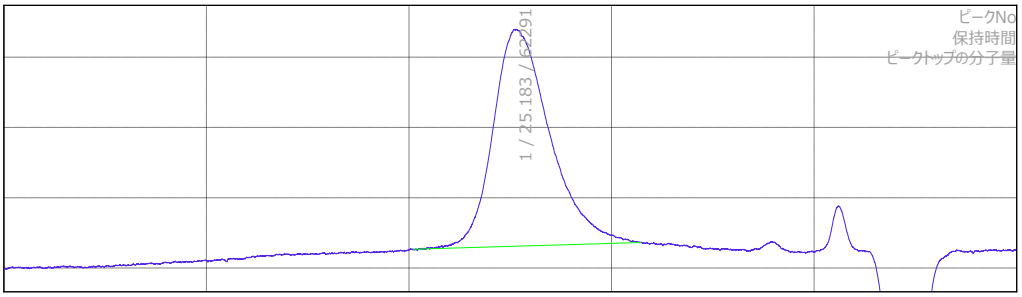

RSLT0005 : 2015-10-20(2).chd : wfz-40
: クロマト RI (-0.671 - 7.473 [mV])

- RI - Mn: 33191 Mw: 61483 Mz: 109368 Mw/Mn: 1.852

Fig. S28. GPC trace of the poly(4-octene) obtained with **6**-MMAO at 20 ℃ for 2 h (entry 8, Table 1).

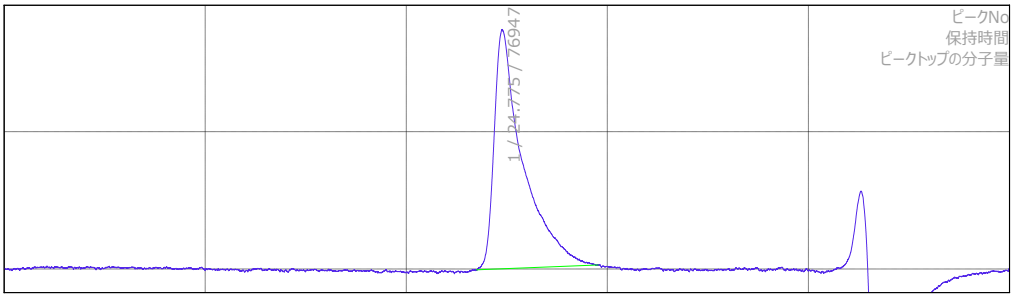

RSLT0005 : 2015-12-15(2).chd : wfz-poly-4-octece-25oc
: クロマト RI (-0.855 - 9.597 [mV])

- RI - Mn: 45133 Mw: 60044 Mz: 71489 Mw/Mn: 1.330

Fig. S29. GPC trace of the poly(4-octene) obtained with **1**-MMAO at 25 ℃ for 2 h (entry 3, Table 2).

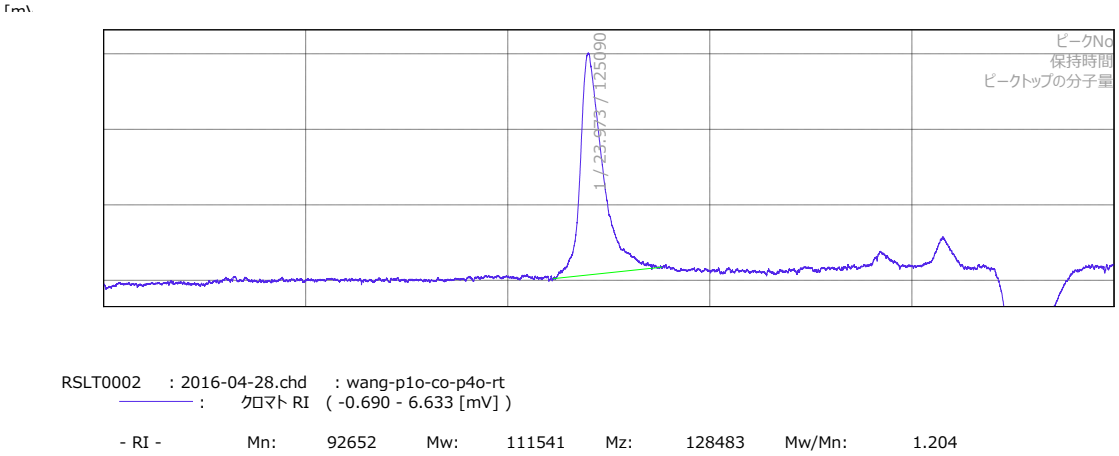

RSLT0002 : 2016-04-28.chd : wang-p1o-co-p4o-rt
: クロマト RI (-0.690 - 6.633 [mV])

- RI - Mn: 92652 Mw: 111541 Mz: 128483 Mw/Mn: 1.204

Fig. S30. GPC trace of the poly(1O-*co*-4O) obtained with **1**-MMAO at 25 ℃ for 2 h (entry 2, Table 3).

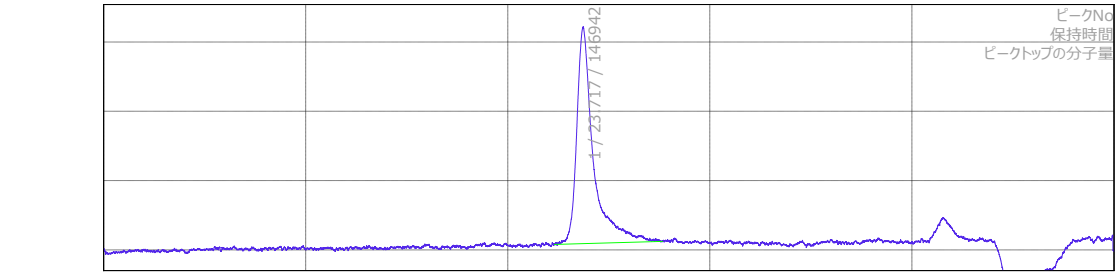

RSLT0001 : 2016-04-28.chd : wang-p1o-co-p4o-rt
: クロマト RI (-0.592 - 7.078 [mV])

- RI - Mn: 107452 Mw: 130015 Mz: 144663 Mw/Mn: 1.210

Fig. S31. GPC trace of the poly(1O-*co*-4O) obtained with **2**-MMAO at 25 ℃ for 2 h (entry 3, Table 3).

7. DSC thermograms of polymers and copolymers

Poly(4-octene)s:

(−25 °C, entry 1, Table 2):

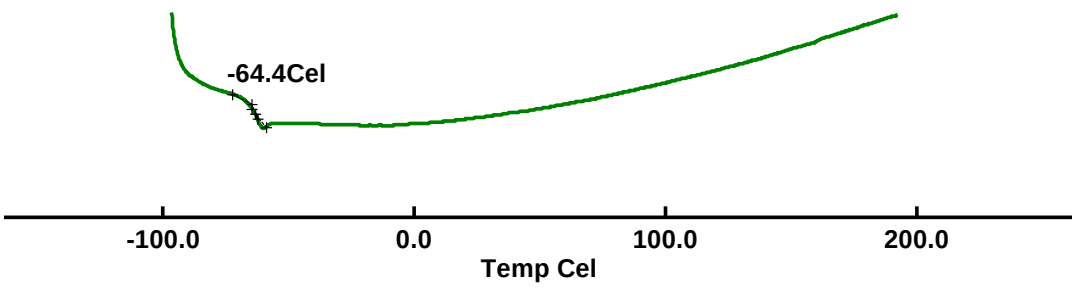

(0 °C, entry 2, Table 2):

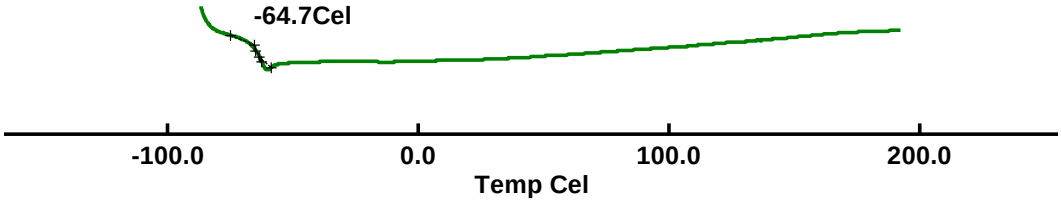

(25 °C, entry 3, Table 2):

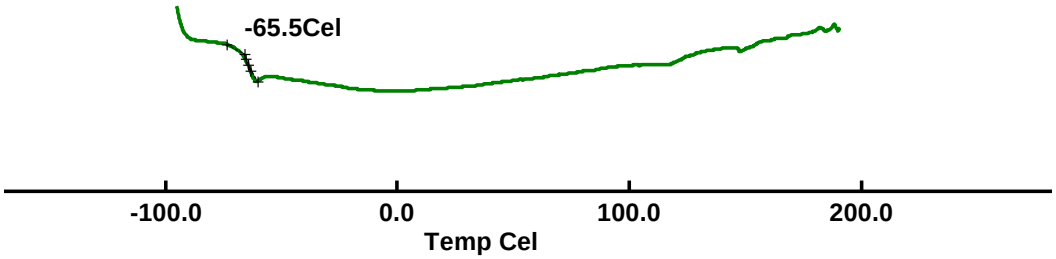

(50 °C, entry 4, Table 2):

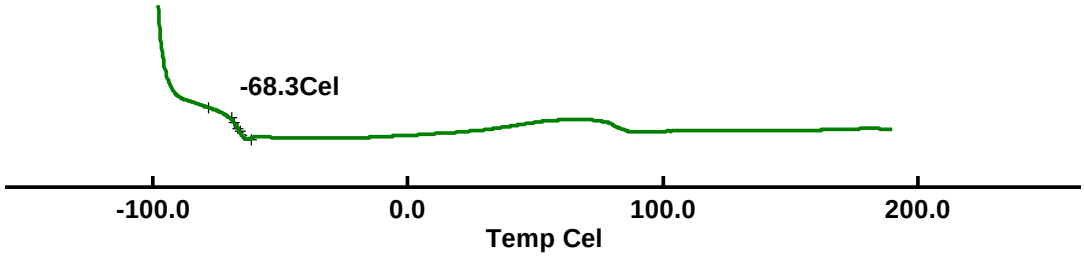

(75 °C, entry 5, Table 2):

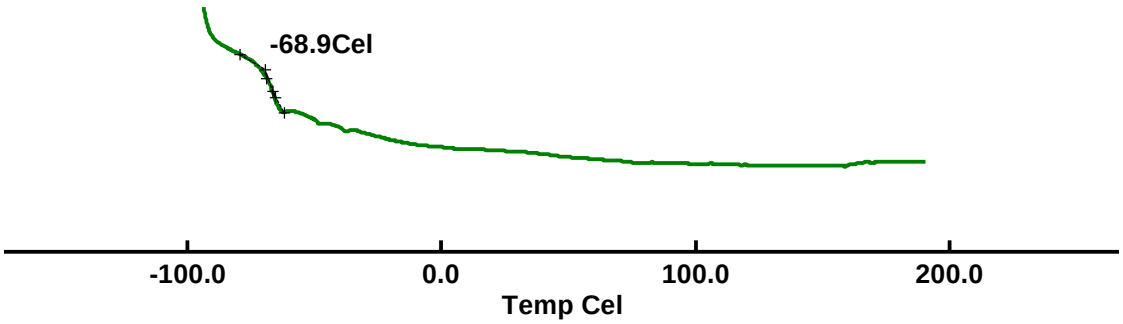

Fig. S32. DSC traces for the poly(4-octene)s obtained with **1**-MMAO at different temperatures (entry 1–5, Table 2).

Poly(2-octene)s:

(0 °C, entry 12, Table 2):

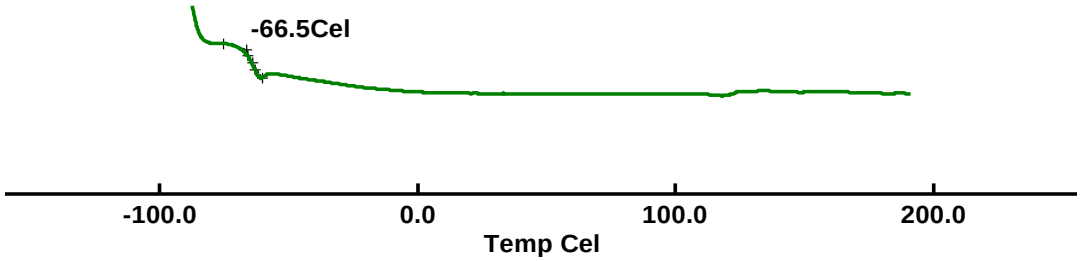

(25 °C, entry 13, Table 2):

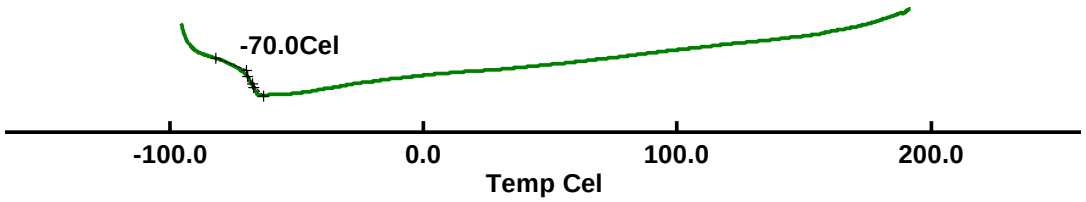

Fig. S33. DSC traces for the poly(2-octene)s obtained with **1**-MMAO at 0 and 25 °C for 2 h (entry 12 and 13, Table 2).

Poly(1-octene)s:

(25 °C, entry 15, Table 2):

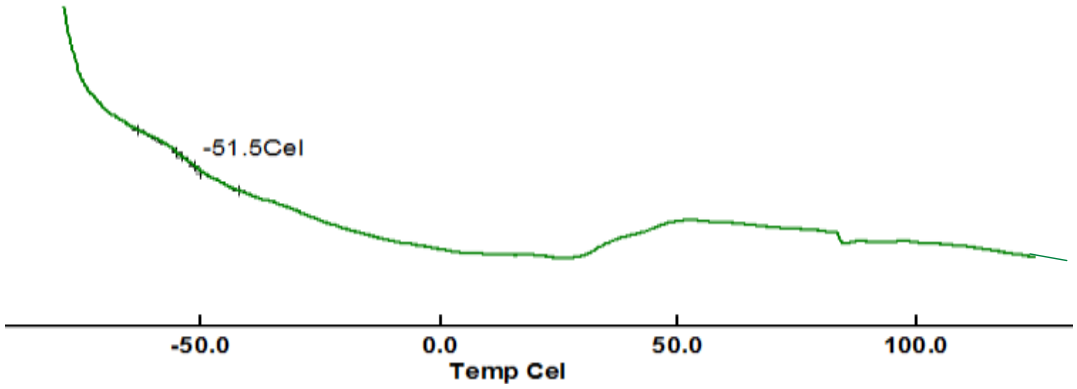

(0 °C, entry 14, Table 2):

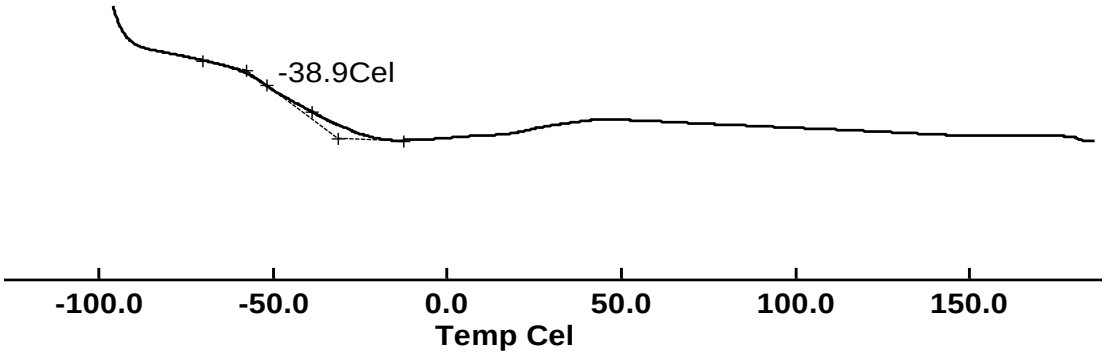

Fig. S34. DSC traces for the poly(1-octene)s obtained with **1**-MMAO at 0 and 25 °C for 2 h (entry 14 and 15, Table 2).

Poly(1O-*co*-4O)s:

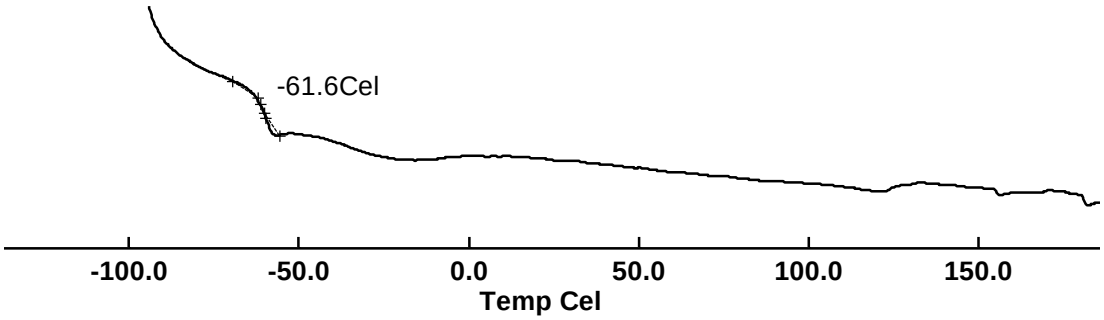

Fig. S35. DSC traces for the poly(1O-*co*-4O) obtained with **1**-MMAO at 25 °C for 2 h (entry 2, Table 3).

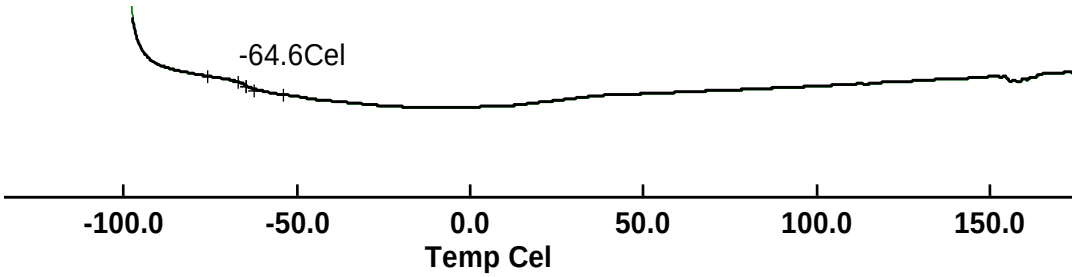

Fig. S36. DSC trace for the poly(1O-*co*-4O) obtained with **2**-MMAO at 25 °C for 2 h (entry 3, Table 3).

Poly(1O-*co*-2O):

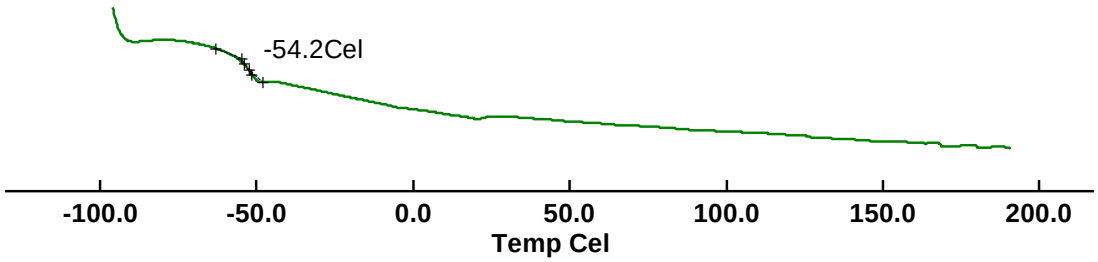

Fig. S37. DSC trace for the poly(1O-*co*-2O) obtained with **1**-MMAO at 25 °C for 2 h (entry 5, Table 3).

References

[1] Wang, F. Z.; Tanaka, R.; Cai, Z. G.; Nakayama, Y.; Shiono, T. *Appl. Organometal. Chem.* **2015**, *29*, 771–776.

[2] Wang, F. Z.; Tanaka, R.; Cai, Z. G.; Nakayama, Y.; Shiono, T. *Macromol. Rapid Commun.* **2016**, *37*, 1375–1381.

[3] Wang, F. Z.; Tanaka, R.; Cai, Z. G.; Nakayama, Y.; Shiono, T. *Polymers* **2016**, *8*, 160–175.